

INFORMATION TO USERS

The most advanced technology has been used to photograph and reproduce this manuscript from the microfilm master. UMI films the text directly from the original or copy submitted. Thus, some thesis and dissertation copies are in typewriter face, while others may be from any type of computer printer.

The quality of this reproduction is dependent upon the quality of the copy submitted. Broken or indistinct print, colored or poor quality illustrations and photographs, print bleedthrough, substandard margins, and improper alignment can adversely affect reproduction.

In the unlikely event that the author did not send UMI a complete manuscript and there are missing pages, these will be noted. Also, if unauthorized copyright material had to be removed, a note will indicate the deletion.

Oversize materials (e.g., maps, drawings, charts) are reproduced by sectioning the original, beginning at the upper left-hand corner and continuing from left to right in equal sections with small overlaps. Each original is also photographed in one exposure and is included in reduced form at the back of the book. These are also available as one exposure on a standard 35mm slide or as a 17" x 23" black and white photographic print for an additional charge.

Photographs included in the original manuscript have been reproduced xerographically in this copy. Higher quality 6" x 9" black and white photographic prints are available for any photographs or illustrations appearing in this copy for an additional charge. Contact UMI directly to order.

U·M·I

University Microfilms International
A Bell & Howell Information Company
300 North Zeeb Road, Ann Arbor, MI 48106-1346 USA
313/761-4700 800/521-0600

Order Number 9000668

Steady state energy transfer processes in laser dye mixtures

Ali, Mohamed, Ph.D.

City University of New York, 1989

U·M·I

300 N. Zeeb Rd.
Ann Arbor, MI 48106

*STEADY STATE ENERGY TRANSFER PROCESSES
IN LASER DYE MIXTURES*

BY


MOHAMED ALI

A dissertation submitted to the Graduate Faculty in Engineering in partial fulfillment of the requirements for the degree of Doctor of Philosophy, The City University of New York.


1989

This manuscript has been read and accepted for the Graduate Faculty in Engineering in satisfaction of the dissertation requirement for the degree of Doctor of Philosophy.

4/18/89
Date


Chair of Examining Committee

4/18/89
Date


Executive Officer

Prof. J. Manassah

Prof. R. Dorsinville

Prof. G. Eichman

Prof. G. Wittman

Supervisory Committee

The City University of New York

ACKNOWLEDGEMENTS

I would like to take this opportunity to acknowledge my deep appreciation to my thesis advisor: Professor Samir Ahmed for his patient guidance, continued encouragement, and numerous invaluable suggestions and discussions during the course of this research.

I am also grateful to Prof. Jamal Manassah and Prof. R. Dorsinville for their valuable theoretical assistance.

My thankfulness goes to my fellow graduate students for their assistance, providing laughter and sunshine during my stay at CCNY.

Finally, none of this would have been possible without my wife constant encouragement, patience, moral support and love.

*TO MY WIFE FATIMA, MY SON AMIR, AND MY
DAUGHTERS SARA AND IMAN*

TABLE OF CONTENTS

TITLE-----	i
APPROVAL-----	ii
ACKNOWLEDGEMENTS-----	iii
TABLE OF CONTENTS-----	v
LIST OF TABLES-----	viii
LIST OF Figures-----	ix
1. INTRODUCTION-----	1
1.2 Excitation Transfer Mechanisms-----	4
1.3 References-----	6
2. RADIATIVE TRANSFER-----	7
2.1 Introduction-----	7
2.2 Fluorescence spectrum of Dye mixtures-----	9
2.3 Accuracy of the Result-----	10
2.4 References-----	12
3. NON RADIATIVE TRANSFER-----	13
3.1 Introudction-----	13
3.2 The First (Standard) Model-----	15
3.3 Forster Kinetics-----	16
3.3.1 Background-----	16
3.3.2 Transfer Efficiency for a Delta pulse Excitation-----	20

3.3.3	Transfer efficiency for steady state illumination-----	22
3.4	Fluorescence spectrum of Dye mixtures-----	32
3.4.1	Introduction-----	32
3.5	Diffusion-controlled or stern volmer kinetics	34
3.6	Intermediate kinetics-----	36
3.6.1	Introduction-----	36
3.6.2	General Approach-----	37
3.6.3	Voltz treatment-----	39
3.6.4	The Gosele treatment-----	41
3.7	The Second Model-----	43
3.8	The Third Model-----	46
3.9	References-----	48
4.	THE EXACT SOLUTION-----	50
4.1	Introduction-----	50
4.2	Theory-----	51
5.	COMPUTER SIMULATION OF THE PROBLEM-----	55
5.1	Introduction-----	55
5.2	The First Program-----	56
5.3	The Second Program-----	60
5.4	The Third Program-----	61
5.5	A General Program-----	62
6.	EXPERIMENTAL RESULTS AND ANALYSIS-----	63
6.1	Introudction-----	63

6.2	Experimental Data: Results and Analysis-----	63
6.3	Discussion and Conclusion-----	68
6.4	References-----	77
7.	A Modified General Model-----	78
7.1	Introduction-----	78
7.2	Definition of the joint probability densities	80
7.3	Change of the Probability density due to Diffusion-----	82
7.4	Change of the Probability density due to diffusion controlled reaction-----	83
7.5	Change of the Joint probability density due to diffusion and Long-Range Energy Transfer----	91
	7.5.1 Mathematical Formulation of the Problem-----	91
	7.5.2 Approximation for long-times-----	95
7.6	Experimental: Comparisons with theory-----	98
7.7	References-----	105
8.	EXPERIMENTAL: RESULTS AND ANALYSIS-----	106
8.1	Introduction-----	106
8.2	Experimental: Results and Analysis-----	107
8.3	References-----	130
9.	SUMMARY AND CONCLUSION-----	131
	APPENDIX-----	134
	BIBLIOGRAPHY-----	137

LIST OF TABLES

6.	-----	63
Table 1:	Transfer efficiency in Naph-DPA solutions -----	72
Table 2:	Transfer efficiency in PPO-DPA solutions -----	73
Table 3:	Transfer efficiency in Rh6G-Ox4 solutions -----	73
Table 4:	Transfer efficiency in RhB-NB solutions -----	73
Table 5:	Transfer efficiency in Naph-Anth acid solutions ---	74
Table 6:	Transfer efficiency in Naph-Biacetly solutions -----	75
Table 7:	Transfer efficiency in Terph-Meth solutions -----	76
7.	-----	78
Table 1:	Transfer efficiency in Naph-DPA solutions -----	100
Table 2:	Transfer efficiency in PPO-DPA solutions -----	101
Table 3:	Transfer efficiency in Rh6G-Ox4 solutions -----	101
Table 4:	Transfer efficiency in RhB-NB solutions -----	101
Table 5:	Transfer efficiency in Naph-Ant acid solutions	102
Table 6:	Transfer efficiency in Naph-Biacetly solutions -----	103
Table 7:	Transfer efficiency in Terph-Meth solutions -----	104

LIST OF FIGURES

8.		106
	Fig. 1: overlap integral of Dich. (donor) and DODC (acceptor)	
	-----	118
	Fig. 2: overlap integral of Dich. (donor) and RhB (acceptor)	
	-----	119
	Fig. 3: fluorescence yield of RhB-Dich. -----	120
	Fig. 4: overlap integral of Coumarine-RhB. -----	121
	Fig. 5: fluorescence yield of Coumarine-RhB. -----	122
	Fig. 6: predicted fluo., absorption and gain of dye mixture:	
	Coumarine-RhB -----	123
	Fig. 7: fluorescence spectra of Coum-ACFV -----	124
	Fig. 8: predicted fluo., absorption and gain of dye mixture:	
	Coumarine-ACFV -----	125
	Fig. 9: fluorescence spectra of R6G-Ox.4 -----	126
	Fig. 10: fluorescence spectra of RhB-N.B. -----	127
	Chart # 1: theoretical calculations for Coum-ACFV -----	128
	Chart # 2: theoretical calculations (rad) for Coum-ACFV -	129

1. INTRODUCTION

It is well known that efficient energy transfer is possible between different dye molecules in solution. In these processes radiative energy is absorbed by one molecule, (the donor), which is thereby raised to an excited state, following which the energy in that excited state is transferred to a lower energy states in a second species of molecules, (the acceptor), which in turn radiates the excitation energy or transfers it to yet another molecule of the same (acceptor) species.

The concept of making practical use of efficient energy transfer processes in dyes has been extended to a number of laser applications. these have included the development of simultaneous output multicolor pulsed dye lasers [1], in which excitation of one dye by the uv output from a pulsed nitrogen laser, is cascaded to two other dyes, and simultaneous laser action obtained in all three.

in fact The subject of energy transfer between unlike molecules in solutions has received considerable theoretical [2-4], as well as experimental attention prior

to the advent of lasers. Different experimental techniques have been used to investigate the nature of excitation transfer in laser dye mixtures.

The concept of energy transfer has been applied [5,6] to improve the pumping efficiency of neodymium lasers. By circulating fluorescent dye solutions between the flashlamp and the laser rod, the light conversion is enhanced since the dyes strongly absorb the visible and uv radiation and then transfer the excitation to the ND ions by emission and reabsorption. Similar improvement in the efficiency of flashlamp-pumped dye lasers has also been reported [7]. Excitation transfer in laser dye mixtures has also been utilized to achieve better dye laser performance at the desired wavelengths. Most studies of excitation transfer in laser dye mixtures has been done by direct measurement of fluorescence lifetime, using nanosecond and picosecond optical pulse excitation and observing the fluorescence decay with a fast electronic detection system [8].

This thesis will show that many fundamental studies can in fact be carried out using steady excitation and measurements of related fluorescence spectra. Furthermore it will be shown that appropriate models can be developed to permit the analytical determination and

prediction of steady state energy transfer and fluorescence, using computer simulation, for dye mixtures. These models and simulation techniques are shown to be appropriate to the effective analysis and handling of the dominant transfer mechanisms responsible for intermolecular energy transfer, including the selection of the most appropriate specific transfer mechanism model for different physical conditions.

It is believed that the approach developed permits effective basic studies to be carried out under relatively simple steady state conditions, and permits relatively simple theoretical predictions to be made for the fluorescence of dye mixtures, and for laser gain when these mixtures are used as lasing media. It is also expected that the approach developed here will produce results of considerable interest to the operation of continuous output dye lasers, and result in improvements of output, efficiency, and threshold pump requirements.

Finally, the validity and range of applicability of these models will be tested, by carrying out a comprehensive and wider ranging set of comparisons between experimental data and theoretical predictions according to these models.

1.2 EXCITATION TRANSFER MECHANISMS

The main mechanisms studied in this work for intermolecular singlet-singlet electronic energy transfer from excited donor molecules (D^*) to acceptor molecules (A), are

(a) A radiative transfer process, in which the fluorescence photons emitted by D^* are absorbed A.

(b) A non-radiative transfer process, due to coulombic interaction between D^* and A, which may be expressed as a multipole-multipole series in which dipole-dipole term is dominant for allowed electronic transitions.

(c) A non-radiative transfer process, due to short-range electron-exchange interaction.

(d) A non-radiative diffusion-controlled collisional transfer.

The energy transfer from donor to acceptor may also be influenced by donor-donor energy migration by one or more of the following processes :

(e) A radiative migration process, in which the fluorescence photons emitted by D^* are absorbed by unexcited donor molecules D.

(f) A non-radiative migration process, due to coulombic multipole-multipole interaction between D^* and D.

(g) A non-radiative migration process, due to short-range electron-exchange interaction between D^* and D .

(h) A non-radiative collisional migration process, due to excimer formation and dissociation.

If the solution is fluid the energy transfer is also influenced by the following :

(i) Diffusion of D^* and A .

1.3 REFERENCES

- [1] AHMED. S, GERGELY. J.S, and INFANTE. D, 1974, J. Chem. Phys. 61, 1548.
- [2] FORSTER, T., 1959, Discuss. Faraday Soc., 27,1.
- [3] FORSTER, T., 1948, Annln. Phys., 2, 55.
- [4] DEXTER, D. L., 1953. J. Chem. Phys., 21, 836.
- [5] URISU, T., and KAJIYAMA, K., 1976, J. Appl. Phys., 47, 3563.
- [6] SEBASTIAN, P. J., 1980, Optics Commun., 35, 113.
- [7] LIN. C, and DIENES, 1973, J. Appl. Phys. 44, 5050.
- [8] LU. P. Y, YU. Z. X, ALFANO. R. R, and GERSTEN. J. I, 1982, Phys. Rev. A 26, 3610.

CHAPTER 2

RADIATIVE TRANSFER

2.1 INTRODUCTION

Singlet-singlet radiative transfer is due to the absorption of a fraction α of the D* fluorescence photons by a molar concentration [A] of a different molecular species. Its probability is given approximately by [1].

$$\alpha = 2.3 \times [A] \int_0^{\infty} F_d(\mu) E_a(\mu) d\mu \quad (2.1.1)$$

Where x is the specimen thickness, [A] is the acceptor molar concentration in M (moles/litre) and the integral describes the overlap of the D* fluorescence spectrum $F_d(\mu)$, normalized to unit area on a wave number scale, and the A absorption spectrum $E_a(\mu)$.

It should be clear that in deriving Eq. (2.1.1) it has been assumed that, $2.3 \times [A] E_a \ll 1$. In general, the fraction (α) of the D* fluorescence absorbed by the acceptor at any given frequency, μ_1 , is given by:

$$\alpha(\mu_1) = F_{od}(\mu_1) \{ 1 - \exp [-2.3 [A] \times E_a(\mu_1)] \} / F_{od}(\mu_1) \quad (2.1.2)$$

Integrating Eq. (2.1.2) over all frequencies, we get:

$$\alpha = \int_0^{\infty} \frac{F_{od}(\mu) \{ 1 - \exp [-2.3 [A] \times E_a(\mu)] \} d\mu}{F_{od}(\mu) d\mu} \quad (2.1.3)$$

or equivalently:

$$\alpha = 1 - \int_0^{\infty} \frac{F_{od}(\mu) \exp [-2.3 [A] \times E_a(\mu)] d\mu}{F_{od}(\mu) d\mu} \quad (2.1.4)$$

2.2 FLUORESCENCE SPECTRUM OF DYE MIXTURE

The donor fluorescence intensity F_{od} in the absence of acceptor is given by:

$$F_{od} = I_0 \{ 1 - \exp [-2.3 [D] X E_d] \} \Phi_{od} \quad (2.2.1)$$

Where $[D]$ is the donor molar concentration.
 X is the specimen thickness.
 E_d is the molar decadic extinction coefficient of the donor
 Φ_{od} is the quantum yield of the donor in absence of acceptor.
 I_0 is the intensity of the exciting light.

The fluorescence intensity of the acceptor F_a (assuming negligible direct excitation of the acceptor) in the presence of the donor is given by:

$$F_a = \alpha F_{od} \Phi_{oa} \quad (2.2.2)$$

Where Φ_{oa} is the quantum yield of the acceptor in the absence of the donor.

The fluorescence intensity of the donor F_d in the presence of the acceptor is given by:

$$F_d = F_{od} - F_{od} [1 - \exp (-2.3 [A] \times E_a)]$$

(2.2.3)

The total fluorescence of the dye mixture assuming that the radiative transfer is the only mechanism responsible for energy transfer is given by:

$$F_t = F_d + F_a = F_{od} [\phi_{oa} \alpha + \exp(-2.3 [A] \times E_a)]$$

(2.2.4)

2.3 ACCURACY OF THE RESULT

Since there are many different processes of energy transfer which might compete with the radiative process, one has to attempt to eliminate most of these processes before using equation (2.2.4) to calculate the total fluorescence intensity some of these are :

- i- Radiative migration (self absorption) there is commonly an overlap of the 0-0 bands of the fluorescence and absorption spectra of the donor . The spectral overlap may be considerable and lead to self-absorption of part of the fluorescence emission,
- ii- Non radiative transfer, (will be discussed in details in the next section).

iii- Concentration quenching. The increase of the donor molar concentration causes a decrease in the molecular fluorescence quantum yield . This self quenching of the donor fluorescence is due excimer formation.

From the above discussion, it is clear that, in order to get the most accurate result for the fluorescence, from equation (2.2.4). (If it is assumed that the radiative transfer is the only mechanism responsible for energy transfer and that the quenching of the donor quantum yield is just due to energy transfer from the donor to the acceptor.) is to :

a- Choose a donor with a negligible overlap between its absorption and fluorescence spectra.

b- Donor and acceptor solution has to be dilute.

c- Observe the fluorescence in reflection, i.e. from the surface excited by the incident radiation.

Clearly choice (a) and (c) should minimize self absorption, while choice (b) would also minimize self absorption and self quenching, it would also minimize any contribution from the radiationless transfer mechanism.

2.4 REFERENCES

- [1] BIRKS. J. B, 1970, Photophysics of aromatic molecules
(Willey, New York,.

CHAPTER 3

NON RADIATIVE TRANSFER

3.1 INTRODUCTION

In this chapter a review of the main mechanisms for singlet-singlet non-radiative energy transfer will be presented. Three different theoretical models will be developed.

The first Model examined assumes that energy transfer mechanisms may be divided into three kinetic regimes: Stern-Volomer kinetics, Forster kinetics, and Intermediate kinetics with the appropriate kinetics being selected in accordance with Birks' selection criteria [6-9].

The second Model assumes that energy transfer mechanisms may be divided into two kinetic regimes: pure diffusion, and combined diffusion and long-range (resonance) interactions, with the appropriate kinetics being selected in accordance with Gosele's selection criteria.

The third Model (Gosele's generalized Model), which does not rely on selection criteria, and which is intended to apply over the whole range of diffusion and resonance energy transfer parameters which could be expected in quenching experiments.

The validity and range of applicability of these models will be tested by carrying out a comprehensive and wider ranging set of comparisons between experimental data and theoretical predictions according to these models.

To carry out these comparisons, the required analytical expressions for the radiationless transfer efficiency, f_{nr} , were first derived, for both δ - pulse and steady state excitations, (interestingly, the same expressions for the transfer efficiency applies for either steady state or δ - pulse excitation), for each of the models examined and for the different experimental regimes being compared. These were then compared with the equivalent experimental data. Results and conclusions of these comparisons will be discussed in chapter 6.

Finally a general approach for determining the fluorescence of dye mixtures will be introduced .

3.2 THE FIRST (STANDARD) MODEL

The studies of energy transfer, according to that model, can be divided into three kinetic regimes:

1. Diffusion-controlled or Stern-Volmer kinetics. are only applicable to the energy transfer process when the rate of statistical mixing due to diffusion and /or excitation migration exceeds the energy transfer rate (complete statistical mixing of D^* and A), so that the energy transfer rate parameter K_t is independent of time. Under these conditions, if the system is excited at time $t=0$ by a δ -function light pulse which yields an initial molar concentration of $[D^*]_0$ excited donor molecules, the subsequent decay of $[D^*]$ is exponential, i.e. K_t is independent of t .

2. Forster kinetics. If D^* and A remain effectively stationary, apart from possible Brownian rotation, during the energy transfer; the energy transfer rate K_t decreases with increase in t , and the D^* fluorescence decays non-exponentially, corresponding to a departure from Stern-Volmer kinetics.

3. Intermediate kinetics, due to the partial mixing of D^* and A by diffusion during the energy transfer.

It is clear that both Stern-Volmer and Forster kinetics are two limiting cases of the precise theory accounting

for the influence of diffusion of molecules on the kinetics of the transfer. Hence in the third case the so called intermediate kinetics which need to be dealt with caution and detail.

3.3 FORSTER KINETICS

3.3.1 BACK GROUND

The total electrostatic interaction between excited states of the donor and acceptor molecules is usually separated into coulomb and exchange terms [1]. In the coulomb term the electrostatic potential can be replaced by a multipole expansion, the leading term of which is the dipole-dipole term. The dipole-dipole interaction is a function of distance R as R^{-3} , and the probability of transfer is the square of this quantity, or R^{-6} . This interaction term is dominant if the transition in the donor and acceptor are allowed. On the other hand, if the transition in the acceptor is spin forbidden, the dipole-dipole term is very small and other interaction terms such as the dipole-quadrupole term and/or the exchange mechanism may be the major contributors to the transfer. A detailed theory of electronic energy transfer has been

developed by Forster [2] in terms of a resonance dipole-dipole interaction mechanism. In the above mechanism, the transitions are coupled to each other as well as to the radiation field. It was shown by Forester that the rate constant for dipole-dipole energy transfer between a donor D and an acceptor A, separated by a distance R could be written as

$$K_t = \frac{1}{T_{od}} \left[\frac{R_o}{R} \right]^6 \quad (3.3.1)$$

Where T_{od} is the excited donor lifetime in the absence of acceptors, and R_o is the critical transfer distance at which the transfer rate (K_t) is equal to the decay rate of the donor in the absence of acceptor. At this distance, one half of the donor molecules decay by energy transfer and one-half decay by the usual radiative and non radiative rates. R_o is related to the spectral overlap of D and A by the equation

$$R_o = \frac{9000 \ln 10 K^2 \phi_{od}}{128 \pi^5 n^4 N} \int_0^{\infty} F_d(\mu) E_a(\mu) / \mu^4 d\mu \quad (3.3.2)$$

Where N is Avogadro's number, n is the refractive index of the solvent, $F_d(\mu)$ is the donor fluorescence intensity (normalized to unit area on a wavenumber scale), $E_a(\mu)$ is the acceptor molar decadic extinction coefficient at wavenumber, Φ_{od} is the donor quantum yield in the absence of acceptor, and K^2 is a molecular orientation factor, which is equal to $(2/3)$ for random orientation due to Brownian rotation.

The approximate criterion for the applicability of the Forster kinetics will be taken as, $r < R_0$.

The assumptions made in the development of Eqs. (3.3.1) and (3.3.2) are as follows:

1. The molecules (dipoles are assumed to be point molecules. This is not a limitation as long as R_0 is much larger than molecular dimensions.
2. The distance between the donor and acceptor is assumed to be larger than molecular dimensions and does not change during lifetime of the excited donor.
3. Contributions from higher multipoles and exchange interactions are neglected.
4. It is assumed that there is no medium or solvent interaction other than dielectric shielding.

5. Thermal equilibrium is assumed to be established between the vibrational modes of the excited donor before transfer takes place. The possibility of energy transfer from higher vibrational or electronic states is ignored.
6. The transitions in both donor and acceptor are assumed to be allowed.
7. The fluorescence and absorption spectra are assumed to be continuous because of collision broadening.
8. The oscillator strength of the donor transition is assumed to be independent of the distribution and number of the acceptor molecules.
9. The rates of transfer between an excited donor molecule and all the acceptor molecules are assumed to be additive.
10. In the transfer of excitation energy from a donor to an acceptor, the possibility of another acceptor being in the path of the interaction is ignored. This may be an important consideration at high concentrations or in intramolecular energy transfer in proteins.
11. Although the acceptor cannot occupy the space of the donor, no correction is made for this limitation.
12. The number of excited donors or acceptors is assumed to be much smaller than the number of unexcited donors or acceptors.
13. The excited donors are assumed to be randomly distributed with respect to the acceptors.

14. The donor-donor interaction is assumed to be negligible. This places a limitation on the donor concentration and eliminates excimers.

3.3.2 TRANSFER EFFICIENCY FOR A δ PULSE EXCITATION

We now consider a solution containing both donors and acceptors, each randomly distributed throughout the solution. It is informative and important to note that both the time-resolved decays of donor fluorescence and the relative quantum yields of the donor are complex functions of the acceptor concentration. Specifically, for a δ -pulse excitation the time-resolved decay of the donor is [3-5].

$$I_d(t) = I_d(0) \exp \left[\frac{-t}{T_{od}} - 2\Omega \left[\frac{t}{T_{od}} \right]^{1/2} \right] \quad (3.3.3)$$

Where $\Omega = [A]/[A]_0$ and

$$[A]_0 = 3000/2 \pi^{3/2} NR_0^3$$

The transfer quantum efficiency f_{nr} is related to the donor fluorescence response function $I_d(t)$ by the equation

$$f_{nr} = 1 - \frac{\phi_d}{\phi_{od}} = 1 - \frac{1}{T_{od}} \int_0^{\infty} \frac{I_d(t)}{I_d(0)} dt \quad (3.3.4)$$

Where ϕ_d is the donor quantum yield in the presence of acceptor.

Substituting (3.3.3) in (3.3.4) yields

$$f_{nr} = \sqrt{\pi} \Omega \exp(\Omega)^2 (1 - \text{erf}\Omega) \quad (3.3.5)$$

where:

$$\text{erf}(X) = \frac{2}{\sqrt{\pi}} \int_0^X \exp(-t^2) dt$$

3.3.3 TRANSFER EFFICIENCY FOR STEADY STATE ILLUMINATION

The complex decay of donor fluorescence reflects the time-dependent population of D-A pairs. Those donors with nearby acceptors decay more rapidly, and donors more distant from acceptors decay more slowly. The complexity of the system is further illustrated by noting that equation (3.3.3) is only strictly true for a δ -pulse excitation. If continuous illumination is used, and turned off at $t = 0$, the decay law is different. This is because one obtains a different starting population using continuous versus δ -pulse excitation. The δ -pulse excitation gives a random sampling of donors. The steady state population of donors is enriched in the more widely spaced D-A pairs.

In this section we develop an expression for the donor decay law under steady state illumination, from which we derive an expression for the transfer efficiency, interestingly we obtain the same expression we had before in the case of a δ -pulse excitation.

Consider a system that consists of N_d unexcited donors and N_a unexcited acceptors as being composed of donor configurations. For example, configuration β includes all donors that have the same acceptor surroundings and

therefore have the same probability of decay when excited. By the configuration β it is meant that all members of class β have an acceptor at positions R_1, R_2, \dots, R_{N_a} , where the positions of the acceptors refer to the donor being considered. In the present treatment, it is assumed that the numbers of excited donor and excited acceptor molecules are much smaller than the respective numbers of unexcited donors and acceptors, and that the unexcited donors and unexcited acceptors are distributed randomly. In addition, energy transfer and interactions between donors are neglected. The probability $P(R_1, R_2, \dots, R_{N_a}) dR_1 dR_2 \dots dR_{N_a}$ of finding a donor molecule (belongs to class β) surrounded by N_a acceptor molecules distributed in a specified fashion, i.e., N_{a1} in the range R_1 to $R_1 + dR_1$, N_{a2} in the range R_2 to $R_2 + dR_2$, etc., is given by the expression

$$P(R_1, \dots, R_{N_a}) dR_1 \dots dR_{N_a} = \prod_{i=1}^{N_a} \frac{4 \pi R_i^2}{V} dR_i \quad (3.3.6)$$

Where V is the volume of the vessel, and R_i is the distance between acceptor i and a donor. The number of donor molecules (N_β) surrounded by acceptor molecules distributed in the above manner is given by

$$N_\beta = N_d \prod_{i=1}^{N_a} \frac{4 \pi R_i^2}{V} dR_i \quad (3.3.7)$$

The rate equation for excited donors belonging to class β is given by:

$$\frac{dn_\beta^*}{dt} = K_1 N_\beta - \left[(T_{od})^{-1} + K_\beta \right] n_\beta^* \quad (3.3.8)$$

Where n_β^* is the number of excited donors at the time t belonging to class β , K_1 is the collection of constants which includes the donor absorption coefficient (assumed to be the same for all donors) and the incident light intensity, N_β is the total number of donors that belong to class β , T_{od} is the excited donor lifetime in the absence of acceptor molecules, and K_β is the resonance

transfer rate constant for any excited donor belonging to class β .

The resonance transfer rate constant can be written as

$$K_{\beta} = \frac{1}{T_{od}} \sum_{i=1}^{N_a} \left[\frac{R_o}{R_i} \right]^6 \quad (3.3.9)$$

Where R_o as defined before in equation (3.3.1), and R_i is the distance between acceptor i and a donor of class β . It should be noted that the orientation factor that appears in the complete resonance transfer constant for dipole-dipole coupling has been averaged out in equation (3.3.9) assuming random orientations. The steady state concentration of excited donors belonging to class β is

$$n_{\beta}^*(0) = \frac{K_1 N_{\beta}}{\left[T_{od}^{-1} + K_{\beta} \right]} \quad (3.3.10)$$

After the incident radiation is turned off (at time $t=0$), the decay can be written as:

$$n_{\beta}^*(t) = n_{\beta}^*(0) \exp \left[-t \left[T_{od}^{-1} + K_{\beta} \right] \right] \quad (3.3.11)$$

Where $n^*_\beta(0)$ is the steady-state concentration given in equation (3.3.10). If we substitute equation (3.3.7) and (3.3.10) in (3.3.11) we get

$$n^*_\beta(t) = K_1 N_d \frac{\exp \left[-t \left[T_{od}^{-1} + K_\beta \right] \right]}{\left[T_{od}^{-1} + K_\beta \right]} \prod_{i=1}^{N_a} \frac{4 \pi R_i^2}{V} dR_i \quad (3.3.12)$$

The total number of excited donor molecules at a time t after the incident radiation is turned off is

$$n^*(t) = K_1 N_d \int_{N_a} \dots \int_{N_a} \frac{\exp \left[-t \left[T_{od}^{-1} + K_\beta \right] \right]}{\left[T_{od}^{-1} + K_\beta \right]} \prod_{i=1}^{N_a} \frac{4 \pi R_i^2}{V} dR_i \quad (3.3.13)$$

If one now takes the time derivative of $n^*(t)$ and expresses K_β as given in equation (3.3.9), one obtains the slope of the decay curve. This yields

$$\frac{dn^*(t)}{dt} = -K_1 N_d \exp\left[\frac{-t}{T_{od}}\right] \left[\int_0^{R_v} \exp\left[\frac{-t}{T_{od}} \left[\frac{R_o}{R}\right]^6\right] \frac{4\pi R^2 dR}{V} \right]^{N_a}$$

(3.3.14)

Where R_v is the radius of the vessel. Forster has evaluated the integral appearing in equation (3.3.14) assuming that $(R_o/R_v)^6(t/T_{od}) \ll 1$. Since R_o is much less than R_v , this assumption is good for all times of interest. Equation (3.3.14) then becomes

$$\frac{dn^*(t)}{dt} = -K_1 N_d \exp\left[\frac{-t}{T_{od}}\right] \left[1 - \left[\pi \left[\frac{R_o}{R_v}\right]^6 \frac{t}{T_{od}} \right]^{1/2} \right]^{N_a}$$

(3.3.15)

Since it has been assumed that $(R_o/R_v)^6(t/T_{od}) \ll 1$, Eq. (3.3.15) can be expressed as

$$\frac{dn^*(t)}{dt} = K_1 N_d \exp\left[\frac{-t}{T_{od}} - N_a \frac{R_o^3}{R_v^3} \left[\frac{\pi t}{T_{od}}\right]^{1/2}\right]$$

(3.3.16)

Integrating Eq. (3.3.16) with respect to time gives

$$n^*(t) = K_1 N_d \int_t^{\infty} \exp \left[\frac{-t'}{T_{od}} - N_a \frac{R_o^3}{R_v^3} \left[\pi \frac{t'}{T_{od}} \right]^{1/2} \right] dt' \quad (3.3.17)$$

If $s = t'/T_{od}$, $\Omega = (N_a/2) (R_o/R_v^3) \sqrt{\pi}$, $x = s^{1/2} + \Omega$, then Eq. (3.3.17) can be expressed as

$$n^*(t) = K_1 N_d T_{od} \int_{[(t/T_{od})^{1/2} + \Omega]}^{\infty} 2 [\exp(\Omega^2 - x^2)] (x - \Omega) dx \quad (3.3.18)$$

After carrying out the integration in Eq. (3.3.18) one finds

$$n^*(t) = K_1 N_d T_{od} \left[\exp \left[\frac{-t}{T_{od}} - 2\Omega \left[\frac{t}{T_{od}} \right]^{1/2} \right] - \sqrt{\pi} \Omega \exp(\Omega^2) \phi \right] \quad (3.3.19)$$

Where

$$\phi = 1 - \operatorname{erf} \left[\Omega + \left[\frac{t}{T_{od}} \right] \right]$$

and

$$\operatorname{erf}(X) = \frac{2}{\sqrt{\pi}} \int_0^{\infty} \exp(-y^2) dy$$

The steady-state concentration is directly obtained from equation (3.3.19) by setting $t = 0$. This gives

$$n^*(0) = K_1 N_d T_{od} \left[1 - \sqrt{\pi} \Omega \exp(\Omega^2) [1 - \operatorname{erf}(\Omega)] \right] \quad (3.3.20)$$

Now the donor quantum yield is given by

$$\Phi_d = \frac{K_e n^*(0)}{K_1 N_d} \quad (3.3.21)$$

Substituting $n^*(0)$ from Eq. (3.3.20) into Eq. (3.3.21) gives

$$\Phi_d = K_e T_{od} \left[1 - \sqrt{\pi} \Omega \exp(\Omega^2) [1 - \text{erf}(\Omega)] \right] \quad (3.3.22)$$

Where K_e is the rate constant for donor emission.

The donor quantum yield in the absence of acceptors is

$$\Phi_{od} = \frac{K_e K_1 N_d T_{od}}{K_1 N_d} = K_e T_{od} \quad (3.3.23)$$

Since the transfer efficiency f_{nr} is given by

$$f_{nr} = 1 - \frac{\Phi_d}{\Phi_{od}} \quad (3.3.24)$$

Combining Eqs. (3.3.22) through (3.3.24), one obtains

$$f_{nr} = \sqrt{\pi} \Omega \exp(\Omega^2) [1 - \text{erf}(\Omega)] \quad (3.3.25)$$

Comparing Eqs. (3.3.5) and (3.3.25) one arrive at the conclusion that the transfer efficiency is the same for both the steady- state and δ - pulse excitation.

3.4 FLUORESCENCE SPECTRUM OF DYE MIXTURE

3.4.1 INTRODUCTION

In this section we develop a general analytical expression for the total fluorescence intensity of dye mixture, assuming that energy transfer is due to non-radiative transfer processes, and that any contribution due to the radiative transfer is totally neglected.

The donor fluorescence intensity F_{od} in the absence of the acceptor is given by:

$$F_{od} = I_o \left[1 - \exp(-2.3 [D] \times E_d) \right] \phi_{od} \quad (3.4.1)$$

The fluorescence intensity of the acceptor F_a (assuming negligible direct excitation by the acceptor) in the presence of the donor is given by:

$$F_a = I_o \left[1 - \exp(-2.3 [D] \times E_d) \right] f_{nr} \phi_{oa} \quad (3.4.2)$$

Where f_{nr} is the quantum efficiency of radiationless energy transfer assuming that only one radiationless mechanism is responsible for the transfer.

Dividing Eq. (3.4.1) by (3.4.2) one get

$$F_a = F_{od} f_{nr} \left[\frac{\Phi_{oa}}{\Phi_{od}} \right] \quad (3.4.3)$$

The fluorescence intensity of the donor F_d in the presence of the acceptor is given by:

$$F_d = F_{od} (1 - f_{nr}) \quad (3.4.4)$$

Adding Eqs. (3.4.3) and (3.4.4) one obtain an expression for the total fluorescence intensity F_t

$$F_t = F_{od} \left[f_{nr} \left[\frac{\Phi_{oa}}{\Phi_{od}} \right] + 1 - f_{nr} \right] \quad (3.4.5)$$

3.5 DIFFUSION-CONTROLLED OR STERN-VOLMER KINETICS

In section 3.3 we discussed singlet-singlet energy transfer in solutions of sufficiently high viscosity in which the molecules are either stationary, or the diffusion or donor excitation migration are sufficiently small. Under these conditions dipole-dipole transfer is described by Forster kinetics. We now consider for a similar solution of low viscosity ($R_0 \ll r$), the energy transfer obeys Stern-Volmer kinetics, so that the transfer rate K_{dif} is time independent. The transfer efficiency is given by [10]

$$f_{nr} = \frac{K_{dif} [A]}{K_{dif} [A] + T_{od}^{-1}} \quad (3.5.1)$$

Where K_{dif} is the rate parameter of a diffusion-controlled collision process is given by [11]

$$K_{dif} = 2 \times 10^5 T/\eta \quad (3.5.2)$$

Where η is the solvent viscosity in poise and T is in °K. These relations are applicable when the rate of statistical mixing due to diffusion and / or migration exceeds the energy transfer rate, so that K_{dif} is effectively constant, due to molecular mixing. The approximate criterion for the applicability of Stern-Volmer kinetics will be taken as $r > 3R_0$.

3.6 INTERMEDIATE KINETICS

3.6.1 INTRODUCTION

When the distance between an excited donor, D^* , and unexcited acceptor, A , varies during the life time of the excited state as a result of Brownian motions, the probability for non-radiative energy transfer, cannot be derived from Eq. 3.3.1.

The influence of diffusion on dipole-dipole energy transfer has to be considered by adding a diffusion term to the differential equation for the donor excitation probability. The influence of diffusion on dipole-dipole energy transfer has been treated theoretically by several authors [12-20]. The various approaches may be divided into two broad groups:

- (a) Those of Yokota and Tanimoto [12], Steinberg and Katchalski [13], and Gosele et al [15-17], which are developed from Forster kinetics; and
- (b) Those of Belikova and Galanin [21] and Voltz et al [14], which are developed from diffusion theory and which extrapolate to Stern-Volmer kinetics.

For our purpose We select two of these treatments for discussion here (Voltz and Gosele), based on their results we try to develop analytical expressions for the non-radiative transfer efficiency component f_{nr} , once we get these expressions for f_{nr} , the problem of obtaining the fluorescence intensity for a laser dye mixtures is a straight forward matter, all one has to do is just substitute f_{nr} into Eq. (3.4.5).

The approximate criterion for the applicability of the intermediate kinetics will be taken as $3R_0 > r > R_0$.

3.6.2 GENERAL APPROACH

Each theoretical result considered below permits an expression for the time dependence of the donor concentration $[D^*]$ following instantaneous creation of an initial concentration $[D^*]_0$. The decay function can be written

$$[D^*] = [D^*]_0 \exp(-t/T_{0d}) \exp(-U [A]) \quad (3.6.1)$$

where U is a time-dependent quenching coefficient (due to energy transfer from the donor to the acceptor) and $[A]$ is

the quencher (acceptor) concentration. The donor quantum yield Φ_d in the presence of the acceptor is then

$$\Phi_d = \int_0^{\infty} K_{fd} [D^*] dt / [D^*]_0 \quad (3.6.2)$$

in which K_{fd} is the radiative rate constant for the $[D^*]$ decay. If Φ_{od} is taken as the quantum yield of the donor in the absence of the acceptor, where $\Phi_{od} = K_{fd} T_{od}$ then

$$\frac{\Phi_d}{\Phi_{od}} = (1/T_{od}) \int_0^{\infty} \exp(-t/T_{od}) \exp(-U [A]) dt \quad (3.6.3)$$

which applies also to steady-state observations. Since the non-radiative transfer efficiency f_{nr} is defined as

$$f_{nr} = 1 - \frac{\Phi_d}{\Phi_{od}} \quad (3.6.4)$$

if we substitute Eq. (3.6.3) into (3.6.4) then

$$f_{nr} = 1 - (1/T_{od}) \int_0^{\infty} \exp(-t/T_{od}) \exp(-U [A]) dt \quad (3.6.5)$$

3.6.3 THE VOLTZ TREATMENT

From diffusion theory (Noyes 1961) the rate parameter of a diffusion-controlled collision process is given by:

$$K_{dif} = \frac{4 \pi N D P r_{da}}{1000} \left[1 + r_{da} (\pi D t)^{-\frac{1}{2}} \right] \quad (3.6.6)$$

where r_{da} is the sum of the collision radii and p is the reaction probability per collision. Following Belikova and Galanin [21], Voltz applied (3.6.6) to a diffusion-controlled dipole-dipole energy transfer process, by substituting $r_{da} = R_o$, and $p = 0.5$, since R_o is defined as the critical distance at which the transfer probability is 0.5. The energy transfer rate parameter thus obtained is

$$K_{et} = \frac{2 \pi \tilde{N} D R_0}{1000} \left[1 + R_0 (\pi D t)^{-\frac{1}{2}} \right] \quad (3.6.7)$$

The time-dependent quenching coefficient (U) introduced by Voltz is

$$U = 2\pi\tilde{N}DR_0 t + 4\tilde{N}R_0^2 (\pi Dt)^{\frac{1}{2}} \quad (3.6.8)$$

where $\tilde{N} = N/1000$

Eq. (3.6.8) into (3.6.5) after carrying out the integration we get (see appendix A)

$$f_{nr} = 1 - \frac{K_0}{K_V} + \frac{K_0}{K_V^{3/2}} \sqrt{\pi} A_V \exp(A_V^2/K_V) \left[1 - \operatorname{erf}(A_V/K_V^{\frac{1}{2}}) \right] \quad (3.6.9)$$

where

$$K_V = K_0 + 3.78 \times 10^{21} D R_0 [A]$$

and

$$A_V = 2.134 \times 10^{21} \sqrt{D} R_O^2 \text{ [A]}$$

and as before, to calculate the fluorescence intensity for a laser dye mixtures, we just substitute Eq. (3.6.9) into (3.4.5).

3.6.4 THE GOSELE TREATMENT

Gosele et al. [15-17], obtained an approximate solution, based on an interpolation between the known solutions at short and long times. They showed that when long range resonance transfer dominates, the quenching coefficient is given by:

$$U = 4 \pi D \tilde{N} r_f t + (4/3) \pi^{3/2} \tilde{N} R_O^3 (t/T_{od})^{1/2} \quad (3.6.10)$$

where

$$r_f = 0.676 (R_O^6/T_{od} D)^{1/4} \quad (3.6.11)$$

Eq. (3.6.10) into (3.6.5) we get (see appendix)

$$f_{nr} = 1 - \frac{K_0}{K_g} + \frac{K_0}{K_g^{3/2}} \sqrt{\pi} A_g \exp(A_g^2/K_g) \left[1 - \operatorname{erf}(A_g/K_g^{1/2}) \right] \quad (3.6.12)$$

where

$$A_g = \Omega K_0^{1/2}$$

$$K_g = K_0 + 4\pi D r_f \dot{N} [A]$$

$$K_0 = 1/T_{od}$$

$$\Omega = \frac{[A] R^3_0}{[7.66 \times 10^{-8}]^3}$$

Once again Eq. (3.6.12) into (3.4.5) we obtain the fluorescence intensity for a laser dye mixtures.

3.7 THE SECOND MODEL

This model assumes that energy transfer mechanisms may be divided into two kinetic regimes: pure diffusion, and combined diffusion and long-range (resonance) interactions, with the appropriate kinetics being selected in accordance with Gosele's selection criteria [22,23].

A. Diffusion Kinetics

Gosele et al. [22-24] introduced a dimensionless parameter Z_0 defined as

$$Z_0 = \left[\frac{1}{2 r_{ad}^2} \right] \left[\frac{R_0^6}{T_{od} D} \right]^{\frac{1}{2}} \quad (3.7.1)$$

For the pure diffusion case, The approximate criterion applicable will be taken as, $Z_0 \ll 1$. The time dependent quenching coefficient $U(t)$ is given by the usual expression for pure diffusion [22],

$$U(t) = 4 \pi D r_{ad} \tilde{N} t + 4 \pi r_{ad}^2 \tilde{N} (Dt/\pi)^{\frac{1}{2}} \quad (3.7.2)$$

Following the general approach developed in section 3.6.2 ,
if we substitute Eq. (3.7.2) into Eq. (3.6.5) we get

$$f_{nr} = 1 - \frac{K_0}{K_2} + \frac{K_0}{K_2^{3/2}} \sqrt{\pi} A_2 \exp(A_2^2/K_2) \left[1 - \operatorname{erf}(A_2/K_2^{1/2}) \right]$$

(3.7.3)

where

$$K_2 = K_0 + 4 \pi r_{ad} \tilde{N} [A] D$$

and

$$A_2 = 2 (\pi D)^{1/2} r_{ad}^2 \tilde{N} [A]$$

Note that these kinetics corresponds to the Stern - Volmer kinetic introduced in the first Model.

B. Combined diffusion and long-range interactions

The approximate criterion applicable for this situation will be taken as, $Z_0 \gg 1$. The time dependent quenching coefficient $U(t)$ is given by [22],

$$U(t) = 4 \pi D r_f \tilde{N} t + (4/3) \pi^{3/2} \tilde{N} R_0^3 [t/T_{od}]^{1/2}$$

(3.7.4)

Eq. (3.7.4) into Eq. (3.6.5), gives:

$$f_{nr} = 1 - \frac{K_0}{K_g} + \frac{K_0}{K_g^{3/2}} \sqrt{\pi} A_g \exp(A_g^2/K_g) \left[1 - \operatorname{erf}(A_g/K_g^{1/2}) \right]$$

(3.7.5)

Where

$$K_g = K_0 + 4 \pi D r_f \tilde{N} [A]$$

and

$$A_g = (2/3) \pi^{3/2} \tilde{N} R_0^3 [A] K_0^{1/2} = \Omega K_0^{1/2}$$

Note that these kinetics combine both the Forster and the intermediate kinetic. Therefore as $D \longrightarrow 0$, $K_g = K_0$, Eq. (3.7.5) reduces to

$$f_{nr} = \pi^{1/2} \Omega \exp(\Omega^2) [1 - \operatorname{erf}(\Omega)] \quad (3.3.5)$$

which is exactly the same as the transfer efficiency for the Forster kinetic.

3.8 THE THIRD MODEL (GOSELE'S GENERALIZED MODEL)

Gosele et al. introduced [22] a more generalized theoretical model, which does not rely on selection criteria, and which is intended to apply over the whole range of diffusion and resonance energy transfer parameters which could be expected in quenching experiments.

In this section we derive a general expression for the non radiative transfer efficiency (f_{nr}) valid for all kinetics, over the whole range of Z_0 or D .

Gosele et al [22] introduced a rough approximation for the time dependent quenching coefficient $U(t)$, over the whole range of diffusion and resonance energy transfer parameters in quenching experiments, given by

$$U(t) = 4 \pi D R_{\text{eff}} t \tilde{N} + 8\pi^{1/2} D^{1/2} R_{\text{eff}}^2 t^{1/2} \tilde{N} \quad (3.8.1)$$

where

$$R_{\text{eff}} = r_{\text{ad}} + 0.724 \left[\frac{R_0^6 K_0}{D} \right]^{1/4}$$

Eq. (3.8.1) covers all limiting cases such as:

$D \rightarrow 0,$ $R_0 \rightarrow 0,$ D very large or R_0 very
 large, $t \rightarrow 0,$ $t \rightarrow \infty.$

This equation represents a useful approximation over the whole range of diffusion and resonance energy transfer parameters. Following the general approach developed in section 3.6.2, if we substitute Eq. (3.8.1) into Eq. (3.6.5), we obtain

$$f_{nr} = 1 - \frac{K_0}{K_3} + \frac{K_0}{K_2^{3/2}} \sqrt{\pi} A_3 \exp(A_3^2/K_3) \left[1 - \operatorname{erf}(A_3/K_3^{1/2}) \right] \quad (3.8.2)$$

where

$$K_3 = K_0 + 4\pi D R_{\text{eff}} \tilde{N} \text{ [A]}$$

and

$$A_3 = 4\pi^{1/2} D^{1/2} R_{\text{eff}}^2 \tilde{N} \text{ [A]}$$

3.9 REFERENCES

- [1] DEXTER, D. L., 1953. J. Chem. Phys., 21, 836.
- [2] FORSTER, T., 1959, Discuss. Faraday Soc., 27,1.
- [3] GALANIN. M. D, 1955, Sov. Phys. JETP,1,317.
- [4] BRIKS. J. B, 1948, J.Phys. B (Proc.Phys.Soc.), ser.2,1,946.
- [5] FORSTER, T., 1948, Annln. Phys., 2, 55.
- [6] BIRKS,J.B.,and GEORGHIOUS,S.,1968,J.Phys. B (Proc. Phys. Soc.), ser.2, vol.1.
- [7] BIRKS,J.B.,1968,J.Phys. B (Proc.Phys.Soc.),[2],1,946-57.
- [8] BIRKS,J.B.,and CONTE,J.C.,1968,Proc.R.Soc.A,303,85-95.
- [9] BIRKS,J.B.,GEORGHIOUS,S., and MUNRO,I.H.,1968,J.Phys.,B (Proc.Phys.Soc.),[2],1,266-73.
- [10] BIRKS. J. B, 1970, Photophysics of aromatic molecules (Willey, New York.
- [11] TURRO. NICHOLAS, 1978, modern molecular photochemistry Benjamin,New York.
- [12] YOKOTA. M, and TANIMOTO. O, 1967, J.Phys. Soc. Japan, 22, 779.
- [13] STEINBERG. I. Z, and KATCHALSKI. E, 1968, J. Chem. Phys., 48,2404.
- [14] VOLTZ,R.,et al.,1966 b, J.Chim.Phys.,63,1259-64.
- [15] GOSELE. U, 1978, Spectrosc. Lett. 11, 445.

- [16] GOSELE. U, HAUSER. M, KLEIN. K. A, and FREY. R, 1975, Chem. Phys. Lett. 34,519 .
- [17] GOSELE. U, and HAUSER. M, 1976, Chem. Phys. Lett. 41, 139.
- [18] BUTLER. P. R, and PILLING. M. J, 1979, Chem. Phys. 41, 239.
- [19] GOCHANOUR. C. R, ANDERSEN. H. C, and FAYER. M. D, 1979, J.Chem.Phys. 70, 4254 .
- [20] HAAN. W, and ZWANZING. R, 1978, J.Chem.Phys.68,1879.
- [21] BELIKOVA. T. P, and GALANIN. M. D, 1958, Opt. Spec., 1, 168.
- [22] GOSELE. U, 1978, Spectrosc. Lett. 11, 445.
- [23] GOSELE. U, HAUSER. M, KLEIN. U.K.A, and FREY. R, 1975, Chem. Phys. Lett. 34,519.
- [24] GOSELE. U, and HAUSER. M, 1976, Chem.Phys.Lett.41,139.

CHAPTER 4

THE EXACT SOLUTION

4.1 INTRODUCTION

All the analytical expressions developed so far to determine the total fluorescence for a laser dye mixture, are based on two basic assumptions:

- 1) Energy transfer has always been assumed due to either radiative or non-radiative processes, if radiative transfer is the dominant mechanism responsible for energy transfer, then any contribution due to non-radiative transfer is totally neglected and vice-versa.
- 2) Direct absorption of the incident light by the acceptor was not taken into consideration.

However, In most practical cases one has to take into account contributions due to both radiative and non-radiative transfer and also contributions due to direct excitation of the acceptor. What is needed is a transfer efficiency which takes into account contributions due to both radiative and non-radiative processes, and a modified

expression for the acceptor fluorescence which also takes into account contributions due to direct excitation.

In order to account for these contributions, we modify the expression for the total fluorescence of a laser dye mixture developed in section (3.4).

4.2 THEORY

The fluorescence intensity of a solution containing donor only is given by the expression:

$$F_{od} = I_o \left[1 - \exp[-2.3 E_d(\mu_{ex}) [D] X] \right] \Phi_{od} = Q_1 \Phi_{od} \quad (4.2.1)$$

where

$$Q_1 = I_o \left[1 - \exp[-2.3 E_d [D] X] \right]$$

and μ_{ex} is the wavenumber of donor excitation.

The fluorescence of the donor in the presence of the acceptor is given by:

$$F_d = I_0 \left[1 - \exp \left[-2.3 E_d(\mu_{ex}) [D] X - 2.3 E_a(\mu_{ex}) [A] X \right] \right] \left[\frac{E_d(\mu_{ex}) [D]}{E_d(\mu_{ex}) [D] + E_a(\mu_{ex}) [A]} \right] \left[(1 - f_{nr}) \phi_{od} - f_r \right] \quad (4.2.2)$$

where f_r is the quantum yield of radiative transfer, given by

$$f_r = (1 - f_{nr}) \alpha_{rad} \phi_{od}$$

substituting the value of f_r into Eq. (4.2.2),

$$F_d = Q_2 \left[\frac{E_d(\mu_{ex}) [D]}{E_d[D] + E_a[A]} \right] \left[1 - f_{nr} \right] \left[1 - \alpha_{rad} \right] \phi_{od} \quad (4.2.3)$$

where

$$Q_2 = I_0 \left[1 - \exp \left[-2.3 E_d(\mu_{ex}) [D] X - 2.3 E_a(\mu_{ex}) [A] X \right] \right]$$

and α_{rad} is the fraction of the donor fluorescence absorbed by the acceptor. The ratio of the EC terms measures the

part of the incident light which is absorbed by the donor molecules. $1 - f_{nr}$ gives the fraction of excited donor molecules which do not transfer their energy to the acceptor molecules in a nonradiative manner.

Dividing Eq. (4.2.1) by Eq. (4.2.2) we get,

$$F_d = F_{od} \left[\frac{Q_2}{Q_1} \right] \left[1 - f_{nr} \right] \left[1 - \alpha_{rad} \right] \left[\frac{E_d[D]}{E_d[D] + E_a[A]} \right] \quad (4.2.4)$$

where

$$Q_2/Q_1 = \frac{1 - \exp \left[-2.3 E_d(\mu_{ex}) [D] X - 2.3 E_a(\mu_{ex}) [A] X \right]}{1 - \exp \left[-2.3 E_d(\mu_{ex}) [D] X \right]}$$

The fluorescence F_a of the acceptor in a solution containing both acceptor and donor, when illuminated at the wavelength of donor excitation, is the result of:

- (a) Direct absorption of the incident light by the acceptor.
- (b) Absorption of the fluorescence of the donor, i.e., radiative energy transfer.
- (c) Nonradiative energy transfer from the donor.

The expression for F_a is given by

$$F_a = Q_2 \left[\frac{E_d(\mu_{ex})[D]}{E_d[D] + E_a[A]} \right] f_{nr} \phi_{oa} + Q_2 \left[\frac{E_a(\mu_{ex})[A]}{E_d[D] + E_a[A]} \right] \phi_{oa} + Q_2 \left[\frac{E_d[D]}{E_d[D] + E_a[A]} \right] f_r \phi_{oa}$$

(4.2.5)

$$= \left[\frac{E_d[D](f_{nr} + f_r) + E_a[A]}{E_d[D] + E_a[A]} \right] Q_2 \phi_{oa}$$

(4.2.6)

multiplying the denominator and numerator of Eq. (4.2.6) by $Q_1 \phi_{od}$ we get,

$$F_a = F_{od} \left[\frac{E_d[D](f_{nr} + f_r) + E_a[A]}{E_d[D] + E_a[A]} \right] \left[\frac{Q_2}{Q_1} \right] \left[\frac{\phi_{oa}}{\phi_{od}} \right]$$

(4.2.7)

Finally adding up Eqs. (4.2.4) and (4.2.7) we get the total fluorescence for the dye mixture.

CHAPTER 5

COMPUTER SIMULATION OF THE PROBLEM

5.1 INTRODUCTION

After developing all the analytical expressions required to determine the steady-state fluorescence for a laser dye mixture. Now we turn our attention to the problem of simulating these expressions to get the required theoretical results. Since we have developed three different models, we discuss three different programs (see appendix B), one for each model (provided that non-radiative transfer is the dominant mechanisms being selected). All three programs will also include a subroutine for determining the fluorescence spectra of dye mixtures had radiative transfer been selected as the dominant mechanism for energy transfer.

5.2 THE FIRST PROGRAM

This program corresponds to the first model (provided that non-radiative transfer is the dominant mechanisms being selected). Two sets of input data are available. The first set is the so called standard data (i.e. data available in the literature for individual dye laser) such as:

a) Donor fluorescence spectrum alone (F_{od}), acceptor fluorescence spectrum alone (F_{oa}), donor absorption spectrum $E_d(\mu)$ and acceptor absorption spectrum $E_a(\mu)$.

b) Φ_{od} (donor quantum yield alone), Φ_{oa} (acceptor quantum yield alone), T_{od} (donor life time alone), η (solvent viscosity in cp based on the assumption that the microscopic viscosity is equal to the macroscopic solvent viscosity), n (the refractive index of the solvent), X (the vessel thickness in cm), $[D]$ (donor concentration in moles per liter), and $[A]$ (acceptor concentration in moles per liter).

c) The diffusion coefficient, $D = D_d + D_a$, where D_d and D_a are diffusion coefficients of donor and acceptor respectively. We use the Stokes - Einstein relation:

$$D_d = D_a = \frac{KT}{4a\pi\eta} \quad (5.2.1)$$

where it is assumed that the donor and acceptor interaction radii, $a_d = a_a = a = 3A^\circ$. Assuming $T = 300^\circ\text{K}$, and substituting the a 's values in (5.2.1) we get:

$$D = \frac{21.96 \times 10^{-6}}{\eta} \text{ cm}^2/\text{sec} \quad (5.2.2)$$

where the viscosity η , is in cp.

The analytical expressions developed in chapter 2 (for radiative transfer), and for the first model in chapter 3 (radiationless transfer), required to determine the fluorescence spectra of dye mixture, will be the second set of input data.

On running the program the following steps will be executed:

- 1) Using the S-E relation D is determined.
- 2) Curve fitting techniques (cubic spline) is used to plot $F_{od}(\mu)$, $F_{oa}(\mu)$, $E_a(\mu)$ and $E_d(\mu)$.
- 3) Using trapezoid and gaussian techniques, the areas under the spectra, $F_{od}(\mu)$, $F_{oa}(\mu)$, $E_a(\mu)$ and $E_d(\mu)$ were determined.

4) The area under $F_{Oa}(\mu)$ is made equal to the area under $F_{Od}(\mu)$,

in the following manner:

a) let:

$$W = \frac{\text{area under } F_{Od}(\mu)}{\text{area under } F_{Oa}(\mu)}$$

b) multiplying the area under F_{Oa} by W .

5) Using Eq. (3.3.2) R_0 is determined.

6) The mean diffusion length, r is determined using the formula:

$$r = \sqrt{2D T_{od}}$$

7) The average distance \bar{R}_{da} between the donor-acceptor molecules in the solution is determined by

$$\bar{R}_{da} = \frac{7.347}{\{[D] + [A]\}^{1/3}} \quad \text{in } \text{\AA}$$

where $[D]$ and $[A]$ are in moles/litre.

8) If $R_{da} > R_0$, (i.e. energy transfer is predominantly a radiative process and that any contribution due to a non-radiative transfer processes is not considered), the following steps will be performed:

i) Using Eq. (2.1.1) or Eq. (2.1.4) f_r is determined.

ii) Using Eq. (2.2.2) the fluorescence spectrum of the acceptor, F_a , is plotted. It is important to note that Eq. (2.2.2) is used in a different, but equivalent form:

$$F_a = W F_{oa} \alpha_{rad} \phi_{oa}$$

iii) Using Eq. (2.2.3) the fluorescence spectrum of the donor, F_d , is plotted.

iv) The total fluorescence of the mixture is simply obtained by adding up F_d and F_a .

9) If $R_{da} < R_0$, (i.e. energy transfer is predominantly a nonradiative processes and that any contribution due to the radiative transfer process is not considered), the following steps will be performed:

i) A Comparison between R_0 and r is made.

ii) If $R_0 > r$, (Forster kinetics), then, Eq. (3.3.5) is used to determine f_{nr} , Eq. (3.4.2) is used to plot F_a , Eq. (3.4.4) is used to plot F_d , and finally the total fluorescence spectra of the mixture is simply obtained by adding up F_d and F_a .

iii) If $r > 3R_0$, (Stern-Volmer kinetics), then, same previous steps of part (ii) is repeated with Eq. (3.5.1) replacing Eq. (3.3.5) to determine f_{nr} .

iv) If $3R_0 > r > R_0$, (Intermediate kinetics), then, same steps of part (ii) is repeated twice, with Eqs. (3.6.9) and (3.6.12) replacing Eq. (3.3.5) to determine f_{nr} . Thus we obtain two different spectra for the dye mixture, one corresponds to the Voltz treatment while the other corresponds to the Gosele treatment.

5.3 THE SECOND PROGRAM

The first set of input data (standard data) is exactly the same as the first program. The analytical expressions developed in chapter 2 (for radiative transfer), and for the second model in chapter 3 (radiationless transfer), required to determine the fluorescence spectra of dye mixture, will be the second set of input data.

On running the program, steps 1 through 8 of the first program will be repeated with step # 6 being replaced to find out the dimensionless parameter (Z_0) introduced in Eq. (3.7.1). To calculate Z_0 , the distance of closest approach (r_{da}) between donor and accepto molecules is assumed to be $6A^0$ (a plausible value for the closest approach of two small molecules in solution). For step # 9 if,

$R_{da} < R_0$, the following steps will be performed:

i) If $Z_0 < 1$ (pure diffusion), following the same approach used before in step # 9 of the first program, fluorescence spectra of the dye mixture is determined with Eq. (3.7.3) used to determine f_{nr} .

ii) If $Z_0 > 1$ (combined diffusion and long-range interactions), again same approach is used to determine fluorescence spectra of the dye mixture with Eq. (3.7.5) used to determine f_{nr} .

5.4 THE THIRD PROGRAM

The first set of input data (standard data) is exactly the same as the first and second programs. The analytical expressions developed in chapter 2 (for radiative transfer), and for the third model in chapter 3 (radiationless transfer), required to determine the fluorescence spectra of dye mixture, will be the second set of input data.

On running the program, steps 1 through 8 of the first and the second programs will be repeated with step # 6 being excluded.

For the last step (step # 8), once it is known that $R_{da} < R_0$, same approach is used to determine fluorescence spectra of the dye mixture with Eq. (3.8.2) used to determine f_{nr} .

5.5 A GENERAL PROGRAM

All three programs developed in the previous sections accounted either for radiative, or nonradiative transfer based on selection criteria which determine the dominant mechanisms for energy transfer. This program will be developed to account for the exact solution developed in chapter 4.

CHAPTER 6

EXPERIMENTAL: RESULTS AND ANALYSIS COMPARISONS OF THEORY AND EXPERIMENT

6.1 INTRODUCTION

In this chapter, Experimental data on radiationless energy transfer, covering a wide range of physical conditions, will be compared with predictions developed from the three different theoretical models introduced in chapter 3, to define and determine their respective validities and range of applicability.

6.2 EXPERIMENTAL DATA: RESULTS AND ANALYSIS

Seven different sets of experimental data for quantum efficiency of radiationless energy transfer, reported in the literature [1-5], have been selected for comparisons with theoretical results calculated according to the three models introduced in chapter 3.

The first and second sets of experimental data were reported by Birks et al. [1], where the yield of nonradiative energy transfer was measured for the following pair of dyes

(1) Naphthalene (the donor) and 9,10 diphenylanthracene (the acceptor) in six different solvents with viscosities ranging from $\eta = 0.62$ CP to 68 CP at a fixed donor concentration, $[D] = 0.1$ M and various acceptor concentrations ranging from $[A] = 10^{-4}$ M to 5×10^{-3} M.

(2) 2,5 diphenyloxazole (donor) and 9,10 diphenylanthracene (acceptor) in two different solvents at a fixed donor concentration, $[D] = 0.01$ M and various acceptor concentrations ranging from: $[A] = 10^{-4}$ M to 5×10^{-3} M.

Table 1 lists the values of energy transfer efficiency, f_{nr} , obtained experimentally for different N-DPA solutions, f_{nr} values calculated according to the three theoretical models discussed above are also tabulated. these calculated values for f_{nr} depends on the kinetics selected according to the Birks criteria for the first model, and according to the Gosele criteria for the second model. Whenever it was not clear which kinetics

would be applicable in the second model, i.e. when $1 \gg Z_0 \gg 1$, we have tabulated two values for f_{nr} , one value corresponding to resonance kinetics, while the other value corresponds to Diffusion Kinetics.

Table 2 lists the experimental results [1] and our theoretical calculations for f_{nr} for different PPO-DPA solutions.

The third and fourth sets of experimental data were reported by Alfano et al. [3], where the yield of nonradiative energy transfer was determined for the following pair of dyes :

(1) Rhodamine-6G (donor) and Oxazine-4 perchlorate (acceptor).

(2) Rhodamine-B (donor) and Nile Blue A perchlorate (acceptor).

In both mixtures Ethyleneglycol was used as the solvent at a fixed donor concentration, $[D] = 1.25 \times 10^{-3}$ M and various acceptor concentrations ranging from $[A] = 3.13 \times 10^{-4} - 5 \times 10^{-3}$ M. Tables 3 and 4 lists the experimental results [9] and our theoretical calculations for f_{nr} for the Rh6G-Ox4 and RhB-NB solutions in Ethyleneglycol.

The fifth set of experimental data were reported by Elkana et al. [4], where the yield of nonradiative energy transfer from naphthalene (the donor) to anthranilic acid (the acceptor) was calculated at ten different solvents with viscosities ranging from $\eta = 0.6$ CP to 1000 CP at a fixed donor concentration, $[D] = 5 \times 10^{-3}$ M and various acceptor concentrations ranging from: $[A] = 10^{-3} - 5 \times 10^{-3}$ M.

Table 5 lists the experimental results [4] and our theoretical calculations for f_{nr} for different N-anthranilic acid solutions.

The sixth set of experimental data were reported by Birks et al. [2], where the yield of nonradiative energy transfer from naphthalene (the donor) to biacetyl (the acceptor) was determined at four different solvents with viscosities ranging from $\eta = 0.34$ CP to 172 CP at a fixed donor concentration, $[D] = 5 \times 10^{-3}$ M and various acceptor concentrations ranging from $[A] = 10^{-4} - 5 \times 10^{-3}$ M. Table 6 lists the experimental results [2] and our theoretical calculations for f_{nr} for different N-biacetyl solutions.

Finally the last set of experimental data were reported by Feitelson J. [5], where the yield of

nonradiative energy transfer from P-Terphenyl (the donor) to 9-methylanthracene (the acceptor) was determined at five different solvents with viscosities ranging from $\eta = 0.6$ CP to 68 CP at a fixed donor concentration, $[D] = 5 \times 10^{-4}$ M and acceptors at various concentrations ranging from $[A] = 5 \times 10^{-4} - 5 \times 10^{-3}$ M. Table 7 lists the experimental results [5] and our theoretical calculations for f_{nr} for different PT-9M solutions.

The critical transfer distance R_0 , and the dimensionless parameter Z_0 are included in all tables. It is informative and important to note that in all the experimental data reported here, the donor concentrations were chosen such that, concentration quenching, self-absorption, and migration of the donor excitation, which would increase the effective transfer efficiency, are all absent. All data required for the calculations of f_{nr} values for the three models are obtained from the same reference where the experimental data are reported.

6.3 DISCUSSION AND CONCLUSION

A comparison of the calculated values of f_{nr} for the three models given in tables 1-7 with the corresponding experimental values given in the first row of every table reveals that:

1) When R_0 is high ($R_0 > 30 \text{ A}^\circ$), tables 2-4, it appears that the first (standard) model agrees closely with the experimental data as long as the Forster kinetics is selected and diffusion does not play a major role. The second model gives almost the same results as the first model provided that diffusion effects are not significant, it also appears as though it would overestimate the actual values of f_{nr} when diffusion effects are significant. The third model shows poor agreement with the experimental data and always overestimates the actual values of f_{nr} . Under these conditions where R_0 is high meaning that, $Z_0 \gg 1$, the Gosele criteria are the most appropriate.

2) When R_0 has an intermediate value ($20 \text{ A}^\circ < R_0 < 30 \text{ A}^\circ$), tables 1, 5, and 7, with lower viscosity, and when diffusion plays a major role, the second model appears to agree closely with the experimental data. As the viscosity gets higher, the third model appears to have the edge in getting the closest fit to the experimental results.

In general, at very high viscosity, where energy transfer is expected to proceed according to the theory of Forster, all models including the third model underestimate the actual values of f_{nr} . This may be due to the neglect of higher multipole - multipole terms in the evaluation of R_0 . Obviously the effects of neglecting such terms will be more important when R_0 is small. What is needed is an extension of the Forster theory to allow for the effects of higher multipole-multipole interaction terms on the magnitude of R_0 .

For the less viscous solution, the f_{nr} values, although sensitive to D , are relatively insensitive to R_0 . A careful inspection of all the Z_0 values listed in Table 1 and Table 5 clearly indicates that the Gosele criterion for the applicability of long-range (resonance) kinetics, may be modified to $Z_0 > 1$, and not $Z_0 \gg 1$.

A comparison of the theoretically calculated values for f_{nr} using the first Model (with Stern-Volmer Diffusion kinetics selected) and the second Model, with experimental values (Tables 1 and 5), show that, the second Model, with resonance kinetics selected, gives the best fit with the experimental data. One is then led to

the conclusion that the Birk's criterion, for the applicability of diffusion kinetics can not be considered as a valid general rule. This conclusion is even more accurate when $Z_0 > 2$, and R_0 is large and long-range kinetics contribute significantly to the transfer efficiency.

3) When R_0 is small, with a value between the collisional interaction radius ($R = 5-6 \text{ \AA}^0$) and the electron - exchange interaction radius ($R = 6-12 \text{ \AA}^0$), Table 6, energy transfer should proceed as a diffusion controlled process and long-range mechanism can be expected to have almost no effect on energy transfer.

For lower viscosity solvents, Table 6 shows that, when, for instance, Hexane was the solvent, the diffusion kinetics of the first model, Stern-Volmer, gave the closest fit to the experimental data. When the solvent was benzene, the diffusion kinetics of the second model gave the closest fit to the experimental results.

As the viscosity got higher, all three models, as expected, underestimated the actual values of f_{nr} . The reason for this is that none of the three models includes a term to account for short range electron-exchange

interactions. It is also clear that under these circumstances, the Birk's criterion for the Stern-Volmer diffusion kinetics is not going to be invalidated, since long-range mechanisms do not contribute at all to the transfer efficiency. This is also true for the Gosele diffusion criterion, since $Z_0 \ll 1$ for all values listed in Table 6.

In conclusion, it appears that at lower viscosities, one of the three models presented, will give a fair agreement between experimental data and theoretical predictions. As the viscosity is increased, and the Forster distance, R_0 , is reduced, all three models presented underestimate the experimental data.

The reason for this is that because contributions from additional terms in the dipole expansion and/or short range electron-exchange mechanisms, are not considered in the models. To allow for these, a theoretical model which takes into account contributions from higher multipole-multipole and/or exchange interaction terms is required.

Solvent \ [A] (10^{-3} M)		0.10	0.20	0.30	0.50	1.00	2.00	3.00	5.00
Benzene $\Gamma=0.62$ $Z_0=0.97$ $R_0=24.2 \text{ A}^*$	f_{nr} (exp)	0.170	0.260	0.320	0.430	0.570	0.740	0.810	0.870
	Mod 1(Stern)	0.100	0.176	0.242	0.347	0.515	0.680	0.761	0.842
	Mod 2 >(Diff)	0.150	0.265	0.350	0.470	0.640	0.785	0.846	0.900
	>(Res)	0.140	0.250	0.330	0.460	0.630	0.776	0.840	0.899
	Mod 3	0.276	0.435	0.538	0.663	0.802	0.894	0.929	0.958
Cyclohexane $\Gamma=0.98$ $Z_0=1.2$ $R_0=24.7 \text{ A}^*$	f_{nr} (exp)	0.160	0.270	0.330	0.430	0.590	0.750	0.800	0.880
	Mod 1(Stern)	0.080	0.140	0.200	0.290	0.450	0.620	0.710	0.800
	Mod 2 >(Diff)	0.120	0.215	0.290	0.410	0.580	0.735	0.800	0.880
	>(Res)	0.125	0.220	0.300	0.420	0.590	0.750	0.818	0.884
	Mod 3	0.237	0.385	0.487	0.616	0.767	0.874	0.915	0.948
B(60%) C(40%) $\Gamma=1.57$ $Z_0=1.5$ $R_0=23.4 \text{ A}^*$	f_{nr} (exp)	0.090	0.120	0.220	0.300	0.440	0.570	0.720	0.770
	Mod 1(Stern)	0.036	0.070	0.100	0.157	0.270	0.430	0.530	0.650
	Mod 2 >(Diff)	0.060	0.100	0.160	0.240	0.390	0.560	0.660	0.766
	>(Res)	0.070	0.130	0.190	0.280	0.440	0.610	0.700	0.800
	Mod 3	0.136	0.242	0.325	0.448	0.626	0.777	0.845	0.906
B(30%) C(70%) $\Gamma=5.89$ $Z_0=2.9$ $R_0=23.4 \text{ A}^*$	f_{nr} (exp)	0.050	0.080	0.150	0.190	0.300	0.440	0.520	0.650
	Mod 1(Stern)	0.010	0.020	0.030	0.048	0.090	0.170	0.234	0.337
	Mod 2 >(Diff)	0.017	0.030	0.050	0.080	0.150	0.260	0.350	0.470
	>(Res)	0.030	0.060	0.090	0.140	0.240	0.400	0.500	0.630
	Mod 3	0.056	0.107	0.153	0.234	0.385	0.567	0.671	0.785
B(10%) C(90%) $\Gamma=25.2$ $Z_0=6$ $R_0=23.5 \text{ A}^*$	f_{nr} (exp)	0.040	0.040	0.080	0.080	0.160	0.280	0.390	0.500
	Mod 1(Voltz)	0.010	0.027	0.040	0.060	0.130	0.230	0.310	0.440
	Mod 2(Res)	0.014	0.028	0.042	0.069	0.129	0.234	0.318	0.447
	Mod 3	0.024	0.047	0.069	0.110	0.202	0.345	0.450	0.593
Cyclohexanol(C) $\Gamma=68.0$ $Z_0=10$ $R_0=23.3 \text{ A}^*$	f_{nr} (exp)	0.030	0.040	0.070	0.060	0.120	0.260	0.290	0.440
	Mod 1(Voltz)	0.006	0.013	0.019	0.030	0.060	0.120	0.170	0.260
	Mod 2(Res)	0.009	0.019	0.028	0.045	0.087	0.164	0.230	0.341
	Mod 3	0.015	0.029	0.043	0.070	0.133	0.241	0.329	0.466

Table 1. Transfer quantum efficiency (f_{nr}) in naphthalene (0.1 M) - DPA [A] Solutions

Solvent [A] \ (10^{-3} M)		2	3	4	5	7
Cyclohexane $\eta = 0.98$ $Z_0 = 25$ $R_0 = 35.6 \text{ \AA}^*$	f_{nr} (exp)	0.340	0.440	0.520	0.580	0.700
	Mod 1(Forst)	0.290	0.390	0.480	0.550	0.650
	Mod 2(Res)	0.410	0.530	0.620	0.680	0.760
	Mod 3	0.500	0.620	0.710	0.760	0.830
Cyclohexanol $\eta = 68$ $Z_0 = 205$ $R_0 = 34.8 \text{ \AA}^*$	f_{nr} (exp)	0.280	0.400	0.490	0.540	0.660
	Mod 1(Forst)	0.270	0.370	0.450	0.520	0.630
	Mod 2(Res)	0.280	0.380	0.460	0.530	0.640
	Mod 3	0.310	0.420	0.500	0.570	0.680

Table 2. Transfer quantum efficiency (f_{nr}) in PPO (10^{-2} M) - DPA [A] solutions

Solvent \ [A] (10^{-3} M)		0.313	0.625	1.25	2.50	5.0
Ethyleneglycol $\eta = 26.09$ $R_0 = 56 \text{ \AA}^*$ $Z_0 = 620$	f_{nr} (exp)	16.4 \pm 3	27.2 \pm 3	47.7 \pm 6	72.0 \pm 7	81.5 \pm 9
	Mod 1(Fors)	0.180	0.330	0.530	0.740	0.890
	Mod 2(Res)	0.190	0.330	0.540	0.750	0.900
	Mod 3	0.200	0.360	0.560	0.770	0.920

Table 3. Transfer quantum efficiency (f_{nr}) in Rh6G (1.25×10^{-3} M) - Ox4 [A] solutions

Solvent \ [A] (10^{-3} M)		0.313	0.625	1.25	2.50	5.0
Ethyleneglycol $\eta = 26.09$ $R_0 = 54 \text{ \AA}^*$ $Z_0 = 621$	f_{nr} (exp)	15 \pm 4	20 \pm 1	41 \pm 5	64 \pm 4	81 \pm 6
	Mod 1(Fors)	0.170	0.310	0.500	0.720	0.880
	Mod 2(Res)	0.170	0.310	0.510	0.720	0.880
	Mod 3	0.190	0.330	0.530	0.750	0.900

Table 4. Transfer quantum efficiency (f_{nr}) in RhB (1.25×10^{-3} M) - NB [A] solutions

Solvent \ (A) (10^{-3} M)		5	2	1
Methanol $\Gamma=0.6$ $Z_s=1$ $R_s=22.8 \text{ \AA}^*$	f_{nr} (exp)	0.920	0.830	0.460
	Mod 1 (Stern)	0.810	0.650	0.460
	Mod 2 > (Diff)	0.881	0.745	0.592
	Mod 2 > (Res)	0.886	0.750	0.600
	Mod 3	0.950	0.875	0.769
Tert-Butanol $\Gamma=4.8$ $Z_s=2.9$ $R_s=22.4 \text{ \AA}^*$	f_{nr} (exp)	0.780	0.600	0.450
	Mod 1 (Stern)	0.340	0.170	0.094
	Mod 2 > (Diff)	0.479	0.267	0.154
	Mod 2 > (Res)	0.640	0.510	0.254
	Mod 3	0.767	0.570	0.368
Glycerol $\Gamma=1000$ $Z_s=40$ $R_s=22.4 \text{ \AA}^*$	f_{nr} (exp)	0.390	0.280	
	Mod 1 (Forst)	0.230	0.100	
	Mod 2 (Res)	0.242	0.108	
	Mod 3	0.310	0.141	
Cyclohexanol $\Gamma=65$ $Z_s=9.2$ $R_s=22.2 \text{ \AA}^*$	f_{nr} (exp)	0.530		
	Mod 1 (Vultz)	0.270		
	Mod 2 (Res)	0.341		
	Mod 3	0.468		
Ethylene glycol $\Gamma=17.4$ $Z_s=4.9$ $R_s=23.5 \text{ \AA}^*$	f_{nr} (exp)	0.560		
	Mod 1 (Vultz)	0.465		
	Mod 2 > (Diff)	0.210		
	Mod 2 > (Res)	0.448		
	Mod 3	0.602		
Amyl alcohol $\Gamma=4.3$ $Z_s=2.6$ $R_s=23 \text{ \AA}^*$	f_{nr} (exp)	0.770		
	Mod 1 (Stern)	0.425		
	Mod 2 > (Diff)	0.567		
	Mod 2 > (Res)	0.710		
	Mod 3	0.831		
n-Butanol $\Gamma=2.8$ $Z_s=2.1$ $R_s=22.2 \text{ \AA}^*$	f_{nr} (exp)	0.850		
	Mod 1 (Stern)	0.485		
	Mod 2 > (Diff)	0.624		
	Mod 2 > (Res)	0.726		
	Mod 3	0.850		
Isopropanol $\Gamma=1.95$ $Z_s=1.8$ $R_s=22.6 \text{ \AA}^*$	f_{nr} (exp)	0.840		
	Mod 1 (Stern)	0.580		
	Mod 2 > (Diff)	0.706		
	Mod 2 > (Res)	0.790		
	Mod 3	0.885		
Ethanol $\Gamma=1.2$ $Z_s=1.47$ $R_s=23 \text{ \AA}^*$	f_{nr} (exp)	0.900		
	Mod 1 (Stern)	0.710		
	Mod 2 > (Diff)	0.807		
	Mod 2 > (Res)	0.840		
	Mod 3	0.924		
Isobutanol $\Gamma=4.1$ $Z_s=2.6$ $R_s=23.2$	f_{nr} (exp)	0.760		
	Mod 1 (Stern)	0.440		
	Mod 2 > (Diff)	0.580		
	Mod 2 > (Res)	0.720		
	Mod 3	0.830		

Table 5. Transfer quantum efficiency (f_{nr}) in naphthalene (0.1 M) - anthranilic acid (A) solutions

Solvent \ [A] (10^{-3} M)		0.1	0.5	1.0	3.0	5.0
Hexane $\tau = 0.34$ $R_m = 4.2 \text{ \AA}^*$ $Z_m = 0.01$	f_{nr} (exp)	0.020	0.080	0.155	0.355	0.480
	Mod 1(Stern)	0.015	0.070	0.130	0.310	0.430
	Mod 2(Diff)	0.025	0.110	0.200	0.440	0.566
	Mod 3	0.030	0.130	0.230	0.480	0.600
Benzene $\tau = 0.62$ $R_m = 4.8 \text{ \AA}^*$ $Z_m = 0.02$	f_{nr} (exp)	0.026	0.120	0.210	0.440	0.570
	Mod 1(Stern)	0.020	0.080	0.150	0.350	0.470
	Mod 2(Diff)	0.030	0.130	0.230	0.480	0.600
	Mod 3	0.035	0.150	0.270	0.530	0.650
ISO (50%) C (50%) $\tau = 10$ $R_m = 5.6 \text{ \AA}^*$ $Z_m = 0.07$	f_{nr} (exp)	0.010	0.050	0.090	0.230	0.330
	Mod 1(Stern)	0.003	0.010	0.030	0.080	0.120
	Mod 2(Diff)	0.005	0.025	0.050	0.130	0.200
	Mod 3	0.007	0.035	0.070	0.180	0.275
Liquid paraffin $\tau = 172$ $Z_m = 0.28$ $R_m = 5.9 \text{ \AA}^*$	f_{nr} (exp)	0.005	0.020	0.040	0.120	0.180
	Mod 1(Voltz)	0.00036	0.002	0.004	0.010	0.018
	Mod 2 \rightarrow (Res)	0.00032	0.0016	0.003	0.0095	0.016
	Mod 2 \rightarrow (Diff)	0.0006	0.003	0.006	0.020	0.030
	Mod 3	0.001	0.007	0.014	0.040	0.060

Table 6. Transfer quantum efficiency (f_{nr}) in naphthalene (0.05 M) -
Biacetyl [A] solutions

Solvent \ [A] (10^{-3})		0.5	1.0	2.0	5.0
Cyclohexane $n = 1$ CP $Z_0 = 21$ $R_0 = 28.1 \text{ \AA}$	$f_{nr}(\text{exp})$	0.110	0.170	0.280	0.530
	Mod 1(Forst)	0.040	0.080	0.160	0.350
	Mod 2(Res)	0.070	0.130	0.230	0.450
	Mod 3	0.090	0.170	0.300	0.550
Methanol $n = 0.6$ CP $Z_0 = 19$ $R_0 = 29.7 \text{ \AA}$	$f_{nr}(\text{exp})$	0.120	0.200	0.310	0.540
	Mod 1(Forst)	0.050	0.100	0.190	0.400
	Mod 2(Res)	0.090	0.160	0.290	0.530
	Mod 3	0.120	0.220	0.370	0.640
Iso-Propanol $n = 2.3$ CP $Z_0 = 36$ $R_0 = 29 \text{ \AA}$	$f_{nr}(\text{exp})$	0.100	0.170	0.290	0.530
	Mod 1(Forst)	0.048	0.090	0.180	0.380
	Mod 2(Res)	0.060	0.120	0.220	0.450
	Mod 3	0.080	0.150	0.270	0.520
Tert-Butanol $n = 4.1$ CP $Z_0 = 43$ $R_0 = 28.7 \text{ \AA}$	$f_{nr}(\text{exp})$	0.090	0.200	0.300	0.500
	Mod 1(Forst)	0.045	0.090	0.170	0.350
	Mod 2(Res)	0.050	0.100	0.190	0.390
	Mod 3	0.070	0.130	0.230	0.470
Cyclohexanol $n = 68$ CP $Z_0 = 165$ $R_0 = 27.8 \text{ \AA}$	$f_{nr}(\text{exp})$	0.080	0.140	0.230	0.440
	Mod 1(Forst)	0.040	0.080	0.150	0.330
	Mod 2(Res)	0.040	0.081	0.154	0.332
	Mod 3	0.050	0.090	0.180	0.370

Table 7. Transfer quantum efficiency (f_{nr}) in Terphenyl (5×10^{-4})M - 9 Methylanthracene [A] solutions.

REFERENCES

- [1] BIRKS, J.B., LEITE, M. S. S. C. P., 1970, J. Phys. B: Atom molec. Phys., 3, 513.
- [2] BIRKS, J.B., LEITE, M. S. S. C. P., 1970, J. Phys. B: Atom molec. Phys., 3, 417-24.
- [3] LU. P.Y, YU.Z.X, ALFANO. R.R, and GERSTEN. J.I, 1983, Phys. Rev. A 27, 2100.
- [4] ELKANA, Y., FEITELSON, J., and KATCHALSKI, E., 1968, J. Chem. Phys., 48, 2399-404.
- [5] FEITELSON, J., 1966, J. Chem. Phys., 44, 1500-4.
- [6] BERLMAN. I.B, 1965, Handbook of fluorescence spectra of aromatic Molecules, Academic press, NEW YORK.
- [7] LIN. C, and DIENES, 1973, J. Appl. Phys. 44, 5050.
- [8] LU. P.Y, YU.Z.X, ALFANO. R.R, and GERSTEN. J. I, 1982, Phys. Rev. A 26, 3610.

CHAPTER 7

A MODIFIED GENERAL MODEL

7.1 INTRODUCTION

We have seen that a comparison between the theoretical predictions and the corresponding experimental results, according to the first and second models, have shown that both theoretical approaches for selection criteria, discussed in chapter 3, are, applicable only under certain limiting physical conditions, where energy transfer is due either purely to diffusion, or to dipole-dipole resonance mechanisms. It has also been shown that, in most cases the third generalized Model gave poor agreement with the experimental data and always overestimates the actual values of f_{nr} .

If one tries to avoid complications and uncertainties in the processes of selecting the most appropriate kinetics, then, the use of a generalized model is a must. But since the third Model (Gosele's generalized Model) is inadequate, a modified general Model

which should give a better agreement with experimental data has to be developed.

It is the purpose of this chapter to develop a modified general Model, by trying to introduce an improved expression for the effective interaction radius, R_{eff} , introduced in Eq. (3.8.1).

We derive a general expression for the non radiative transfer efficiency, f_{nr} , for the general case of energy transfer accompanied by diffusion. Our approach will be based on the statistical method of pair probability densities already used with success for diffusion controlled bimolecular reactions [1]. First we introduce the concept of the joint probability distributions then the problem of the kinetics of the diffusion-limited reaction $A + B \rightarrow AB$ will be formulated in terms of the pair probability densities of the reacting particles (every A taken with every B). The differential equation for the alteration of these pair densities due to diffusion, reaction and long range resonance energy transfer will be considered.

Finally the theory will be compared with experiment to test the validity of the Model.

7.2 DEFINITION OF THE JOINT PROBABILITY DENSITIES

In order to avoid mathematical complexities, it will be convenient to restrict the treatment to those cases in which the distributions of the A's and the B's depend only on the distance of each A from each B (and vice versa). The probability distributions will be assumed to be otherwise uniform over the entire medium (i.e., random distributions). As a consequence of their interdependence, it will be necessary to deal with a number of distinct probability distributions. These will be defined as follows:

$PA_i(r_a, t) dV_a / V =$ probability that A_i is in the volume element dV_a at r_a, t .

$PA_i(B_j) (r_a, t, r_b) dV_a / V =$ probability that A_i is in dV_a at r_a, t given that B_j is at r_b, t .

These probabilities may be related to the macroscopic properties of the systems by noting that the macroscopic density of A particles, C_a , is given by

$$C_a(r_a, t) = \frac{1}{V} \sum_i^{\overset{0}{N_a}} PA_i(r_a, t), \quad (7.2.1)$$

where $\overset{0}{N_a}$ is the number of A particles at $t=0$. Similarly,

the average concentration of A's at r_a, t given that B_j is at r_b can be expressed as a sum of the $PA_i(B_j)$'s. Under the assumption that the distributions depend only on the relative positions of

the A's and B's, the PA_i 's are independent of position and are functions of time only. On the other hand, the $PA_i(B_j)$ are functions of r_a, t and of the given position of the B atom, r_b . The corresponding probability distributions of the B_j 's, PB_j and $PB_j(A_i)$ are defined similarly.

By a well-known theorem from probability theory, we may define pair probability distributions:

$$P_{ij} = PA_i(B_j) PB_j = PA_i PB_j(A_i) \quad (7.2.2)$$

such that:

$P_{ij}(r_a, r_b, t) dV_a dV_b / V^2 =$ probability that A_i is in dV_a at r_a, t and that B_j is in dV_b at r_b, t .

This latter probability density is the joint probability distribution for A_i and B_j . The P_{ij} 's may also be related to the macroscopic properties of the system. Consider all of the AB pairs in the system, every A taken with every B. The average number of pairs having the A in dV_a at r_a, t and the B in dV_b at r_b, t is given by:

$$C_{ab}(r_a, r_b, t) dV_a dV_b = \frac{1}{V^2} \sum_i^{N_a^0} \sum_j^{N_b^0} P_{ij}(r_a, r_b, t) dV_a dV_b \quad (7.2.3)$$

It is the purpose of the following sections to show how P_{ij} vary with r_a , r_b and t due to diffusion, reaction and long range resonance energy transfer.

7.3 CHANGE OF THE PROBABILITY DENSITY DUE TO DIFFUSION

Consider the six-dimensional hyperspace formed by the combination of the cartesian laboratory coordinates of A_i and the cartesian laboratory coordinates of B_j . This is the space in which the joint probability density, is properly defined. One desires to find the rate of change of in the hypervolume element $dV_a dV_b$. This rate, is just the change due to the probable flux of A_i and B_j into $dV_a dV_b$ through the hyperfaces of $dV_a dV_b$ plus the change due to the probable rate of destruction of A_i and B_j within $dV_a dV_b$. If one further defines $(dP_{ij} / dt)_{chem}$ as the probable rate at which changes due to the reaction of A_i or B_j in $dV_a dV_b$, and assuming radial symmetry, one obtains:

$$D \left[\frac{d^2 P_{ij}}{dr^2} + \frac{2}{r} \frac{dP_{ij}}{dr} \right] + (dP_{ij} / dt)_{\text{chem}} = dP_{ij} / dt \quad (7.3.1)$$

Where $D = D_a + D_b$, D_a and D_b are the diffusion coefficients of the A's and B's particles respectively.

It should be noted that this differential equation applies only to the region $|r_a - r_b| > r_{ab}$, where r_{ab} is some AB separation within which A and B react and disappear from the system (distance of closest approach). No attractive or repulsive forces are assumed to prevail between the reacting molecules whenever the distance between their centers of mass is greater than r_{ab} .

7.4 CHANGE OF THE PROBABILITY DENSITY DUE TO DIFFUSION CONTROLLED REACTION

One desires to determine the rate of change of P_{ij} in $dV_a dV_b$ caused by the reaction of A_i or B_j . Noting that the pair $A_i B_j$ is destroyed if either A_i or B_j react with any other B or A and that A_i or B_j cannot react with each other in the region in which Eq. (4.4.4) applies ($|r_a - r_b| > r_0$), one concludes that

$$-(dP_{ij}/dt)_{\text{chem}} dt dV_a dV_b/V^2$$

= probability that simultaneously A_i is in dV_a at r_a, t and that B_j is in dV_b at r_b, t and that either A_i reacts with B_k ($k \neq j$) or B_j reacts with A_m ($m \neq i$), during the interval dt .

Since the possibilities of reaction of A_i with each of the B_k are mutually exclusive, we may sum the contributions to the above probability due to the reaction of A_i with each of the B_k ($k \neq j$). The same is true for the reaction of B_j with the A_m ($m \neq i$). The possibility of both A_i reacting with B_k ($k \neq j$) and B_j reacting with A_m ($m \neq i$) simultaneously is not excluded, however, so that a summation of the probabilities for each of the possible reactions is legitimate only if the probability of both particles reacting is negligible with respect to the probability of one reacting. This can be achieved by making dt , dV_a or dV_b arbitrarily small. One can proceed, therefore, to determine the probabilities of the individual reactions and sum them.

The probability that A_i is in dV_a , B_j is in dV_b , and that A_i reacts with a particular B_k during dt may be expressed as a product of probabilities. It is just the

probability that B_j is in dV_b at r_b given that A_i and B_k are reacting in a small volume element at r_a , times the probability that A_i and B_k react irrespective of where B_j is located. The first of these is a conditional triplet probability. It may be approximated by a superposition technique in which one assumes that the correlation between the particles arises owing to the independent interaction of each of the pairs. Since two B particles interact only by volume exclusion and indirectly by their mutual correlation with the A's, one would expect the direct chemical interaction of A_i with the B's to dominate the required triplet probability. One may therefore approximate the probability that B_j is in dV_b at r_b given that A_i and B_k are in a small volume element at r_a by $P_{B_j}(A_i)dV_b/V$ or $(P_{ij}/\bar{P}_{A_i})dV_b/V$. Therefore the required probabilities:

$$\frac{-P_{ij}}{\bar{P}_{A_i}} \frac{dV_b}{V} \left[\frac{d\bar{P}_{A_i}}{dt} \right]_{B_k} dt \frac{dV_a}{V} \quad (7.4.1)$$

where $-[d\bar{P}_{A_i}/dt]_{B_k} dt \frac{dV_a}{V}$ is the probability that A_i and B_k

react in dV_a during dt irrespective of where B_j is located. Summing these probabilities for the reaction of A_i with all B_k ($k \neq j$) and the probabilities for reaction of B_j with all A_m ($m \neq i$), one obtains

$$(dP_{ij}/dt)_{\text{chem}} = f_{ij}(t) P_{ij} \quad (7.4.2)$$

where

$$f_{ij} = \frac{1}{\bar{P}A_i} \sum_{k \neq j}^0 N_b \left[\frac{d\bar{P}A_i}{dt} \right]_{B_k} + \frac{1}{\bar{P}B_j} \sum_{m \neq i}^0 N_a \left[\frac{d\bar{P}B_j}{dt} \right]_{A_m} \quad (7.4.3)$$

Substitution of (7.4.2) into Eq. (7.3.1) yields

$$D \left[\frac{d^2 P_{ij}}{dr^2} + \frac{2}{r} \frac{dP_{ij}}{dr} \right] + f_{ij}(t) P_{ij} = dP_{ij}/dt. \quad (7.4.4)$$

It may be noted that $f_{ij}(t)$ is never positive.

If (7.4.4) can be solved for P_{ij} , one can immediately determine the probable rate of the reaction $A_i + B_j \rightarrow AB$. It is merely the flux of A_i into B_j or vice versa. This flux is given by

$$\left[\frac{d\bar{P}A_i}{dt} \right]_{B_j} = \left[\frac{d\bar{P}B_j}{dt} \right]_{A_i} = \frac{-4 \pi r_0^2 (D_a + D_b)}{V} \left[\frac{dP_{ij}}{dr} \right]_{r_0} \quad (7.4.5)$$

where $r = |r_a - r_b|$ and r_0 is an AB separation outside of which the AB interaction is independent of r , but inside of which the interaction potential rapidly increases to its value for the AB bond. The total rate of the reaction $A+B \rightarrow AB$ is given by

$$\frac{dC_a}{dt} = \frac{dC_b}{dt} = \frac{1}{V} \sum_i N_a^0 \sum_j N_b^0 \left[\frac{dP_{ij}}{dt} \right]_{B_j} = \frac{-4 \pi r_0^2 (D_a + D_b)}{V} \sum_i \sum_j \left[\frac{dP_{ij}}{dr} \right]_{r_0} \quad (7.4.6)$$

The $N_a^0 N_b^0$ differential equations of the form (7.4.4) are coupled through the functions $f_{ij}(t)$. This coupling may be simplified by the substitution

$$P_{ij} = \frac{W_{ij}}{r} \exp \left[\int_0^t f_{ij} dt \right] \quad (7.4.7)$$

The differential equations for the W_{ij} are no longer coupled and become

$$D \frac{d^2 W_{ij}}{dr^2} = \frac{dW_{ij}}{dt} \quad (7.4.8)$$

The problem, therefore, centers around the solution of the equations of the form (7.4.8) with the appropriate boundary conditions. At first sight, it might seem that, even if (7.4.8) were solved, for each of the W_{ij} , Eq.

(7.4.7) could not be solved for the P_{ij} , since the f_{ij} depend on the P_{ij} in a complicated manner. This problem is greatly simplified, however, if one takes advantage of a few facts demanded by the physical situation.

One notes that the differential equations for the P_{ij} are all identical. One expects, therefore that all of the P_{ij} will be the same unless special boundary conditions exist for certain of the pairs. If all of the particles are initially randomly distributed with respect to one another, all of the P_{ij} are identical and the treatment is quite straightforward. In general there will be at most only a very few types of the P_{ij} . In the remainder of this section we shall deal in detail with the case for which all of the P_{ij} are identical.

Another factor which simplifies the solution of (7.4.7) and permits the evaluation of the f_{ij} is that C_{ab} , the sum of the P_{ij} [see Eq. (7.2.3)] must become independent of r for large values of r . Since the system is infinite, this limiting value, $C_{ab}(\infty, t)$, is just the average value over the system. We have, therefore,

$$C_a C_b = C_{ab}(\infty, t) = \frac{1}{v^2} \sum_i^{N_a} \sum_j^{N_b} \exp \left[\int_0^t f_{ij} dt \right] U_{ij}(\infty, t) \quad (7.4.9)$$

where:

$$U_{ij}(r, t) = W_{ij}(r, t) / r \quad (7.4.10)$$

This single equation resulting from the boundary condition on the P_{ij} at large values of r will go a long way toward the determination of the f_{ij} . If all of the P_{ij} are identical, equation (7.4.9) completely determines P_{ij} . In this case, (7.4.9) becomes

$$C_a C_b = C_a^0 C_b^0 U_{ij}(\infty, t) \exp \left[\int_0^t f_{ij} dt \right] \quad (7.4.11)$$

where

$$C_a^0 = N_a^0 / V, \quad C_b^0 = N_b^0 / V \quad (7.4.12)$$

Elimination of f_{ij} from Eqs. (4.4.11) and (4.4.15) leads to:

$$P_{ij} = \frac{C_a C_b}{C_a^0 C_b^0 U_{ij}(\infty, t)} U_{ij}(r, t) \quad (7.4.13)$$

The effect of the coupling due to competition is then simply to supplement the boundary condition at time $t=0$ by a stronger condition requiring P_{ij} to approach $C_a C_b / C_a^0 C_b^0$ at large values of r at all times. One may evaluate C_a and C_b by integrating Eq. (7.4.6) which takes the form

$$\frac{dC_a}{dt} = \frac{dC_b}{dt} = -4 \pi r_o^2 D C_a^o C_b^o \left[\frac{dP_{ij}}{dr} \right]_{r_o} \quad (7.4.14)$$

Taking the derivative of (7.4.13) and substituting into (4.4.14), one obtains

$$\frac{dC_a}{dt} = \frac{dC_b}{dt} = -4 \pi r_o^2 D \frac{C_a C_b}{U_{ij}(\infty, t)} \left[\frac{dU_{ij}(r, t)}{dr} \right]_{r_o} \quad (7.4.15)$$

We restrict ourselves to the case of randomly distributed molecules without initial correlation. Then all P_{ij} and f_{ij} becomes independent of i, j at all times suppressing the subscripts i, j and assuming a boundary condition,

$U(r \rightarrow \infty, t) = 1$, Eq. (7.4.15) reduces to:

$$\frac{dC_a}{dt} = \frac{dC_b}{dt} = -4 \pi r_o^2 D C_a C_b \left[\frac{dU}{dr} \right]_{r_o} \quad (7.4.16)$$

7.5 CHANGE OF THE JOINT PROBABILITY DENSITY DUE TO DIFFUSION AND LONG-RANGE ENERGY TRANSFER

7.5.1 MATHEMATICAL FORMULATION OF THE PROBLEM

Let us assume that after δ - excitation in the volume V there are N_d^0 excited donor molecules which may diffuse and transfer simultaneously their excitation energy with a certain probability by dipole-dipole interaction to some of the N_a^0 (unexcited) acceptor molecules ($N_a^0 \gg N_d^0$). The transferr probability per second depends on the distance r of the interacting donor-acceptor pair and may be written as [2]

$$W(r) = \alpha / r^6$$

where

$$\alpha = R_0^6 / T_{od}$$

We define pair probability densities P_{ij} for the excited donor molecules and the acceptor molecules:

$P_{ij}(r_d, r_a, t) dV_d dV_a / V^2$, is probability of finding at time t the donor D_i ($i=1,2,\dots, N_d^0$) in a volume element dV_d at r_d and the acceptor A_j ($j=1,2,\dots, N_a^0$) in dV_a at r_a .

Taking into account the change in P_{ij} due to, both the transfer probability, $W(r)$, and the decay of the excited donors, Eq.(7.4.4) can be rewritten as:

$$-P_{ij} / T_{od} - W(r) P_{ij} + D \sum P_{ij} - f_{ij}(t) P_{ij} = dP_{ij}/dt \quad (7.5.1)$$

where $f_{ij}(t) P_{ij}$ is the approximate probability change of P_{ij} due to energy transfer from the donor D_i to any acceptor A_k

($k \neq j$) or from any donor D_m ($m \neq i$) to the acceptor A_j .

We assume a solution for Eq. 7.5.1 in the form[1]:

$$P_{ij} = U_{ij}(r,t) \exp \left[- \int_0^t f_{ij}(t) dt - t / T_{od} \right] \quad (7.5.2)$$

We restrict ourselves to the case of randomly distributed donors and acceptors without initial correlation. Then all P_{ij} and f_{ij} becomes independent of i, j at all times suppressing the subscripts i, j , Eq. 7.5.2 reduces to:

$$P(r,t) = U(r,t) \exp \left[- \int_0^t f(t) dt - t / T_{od} \right] \quad (7.5.3)$$

Substituting Eq. 7.5.3 into Eq. 7.5.1 we arrive at the modified differential equation:(see Eq. 7.4.8)

$$dU(r,t) / dt = D \nabla^2 U - W(r)U \quad (7.5.4)$$

Following the same steps introduced in section 7.4, but, with Eq. 7.4.11 modified to:

$$\frac{C_a C_d^*}{C_a^0 C_d^{*0}} = \exp \left[- \int_0^t f(t) dt - t / T_{od} \right] \quad (7.5.5)$$

(C_a^0, C_d^{*0} : initial concentration of acceptors and excited donors respectively after δ - excitation, $C_a \approx C_a^0 \gg C_d^{*0}$) and assuming spherical symmetry we obtain for the concentration C_d of excited donors after δ - excitation (see Eq. 7.4.16)

$$dC_d^* / dt = - C_d^* / T_{od} - C_d^* \Phi(t) \quad (7.5.6)$$

with [3-5]

$$\Phi(t) = 4 \pi r_{ad} D C_a C_b \left[\frac{dU}{dr} \right]_{r_{ad}} + \int_{r=r_{ad}}^{\infty} W(r) U(r,t) dV \quad (7.5.7)$$

The first term of (7.5.7) describes the luminescence quenching of the donors due to direct collisions and the second term that due to long-range energy transfer.

For the determination of $\Phi(t)$ we must solve (7.5.4) with the initial condition for randomly distributed donors and acceptors

$$U(r, t = 0) = 1 \quad \text{for } r > r_{ad}$$

$$U(r = r_{ad}, t) = 0.$$

Eq.(7.5.4) can not be solved analytically in general. Gosele et al. [3-5] have given treatments for long times and for short times as well as interpolation formula, and they have proposed the use of a formal effective radius r_{eff} over the whole range of diffusion and resonance energy transfer parameters (see section 3.8), repeated here for convenience:

$$r_{\text{eff}} = r_{\text{ad}} + r_f \quad (3.8.1)$$

with

$$r_f = 0.676 (\alpha / D)^{\frac{1}{2}}$$

Eq. (3.8.1) is certainly a good approximation for all limiting cases (as for example $D \longrightarrow 0$, or $\alpha \longrightarrow 0$) but is a poor approximation for an intermediate diffusion region ($Z_0 \approx 1$).

A more accurate expression for r_{eff} may be derived from the limiting value of $\Phi(t)$ at long times, Φ_{∞} .

7.5.2 APPROXIMATION FOR LONG TIMES

For long times we may assume steady state conditions for $U(r,t)$: $dU / dt = 0$. Now the normalized distribution function $U(r)$ satisfies the steady state differential equation:

$$D \nabla^2 U - W(r)U = 0 \quad (7.5.8)$$

with the substitution $U = vr^{-\frac{1}{2}}$, $Z = (1 / 2r^2)(\alpha / D)^{\frac{1}{2}}$ and $W(r)$ according to (3.3.1), (7.5.8) may then be written

for spherical symmetry as a modified Bessel differential equation of order 1/4 [4]:

$$z^2 \frac{d^2 v}{dz^2} + z \frac{dv}{dz} - \left[1/16 + z^2 \right] v = 0 \quad (7.5.9)$$

Applying the boundary conditions $U(r \rightarrow \infty) = 1$ and $U(r_{ad}) = 0$, and with $z_0 = (1 / 2r_{ad})(\alpha / D)^{1/2}$ we get the solution of (7.5.9) as

$$U(z) = \frac{z^{3/4}}{\Gamma(1/4)} \left[K_{1/4}(z) - \frac{K_{1/4}(z_0)}{I_{1/4}(z_0)} I_{1/4}(z) \right] \quad (7.5.10)$$

where $K_{1/4}$ and $I_{1/4}$ are modified Bessel functions of order 1/4.

The limiting value of $\Phi(t)$ at long times, Φ_∞ is given by [4]:

$$\Phi_\infty = 4 \pi r_{ad} D C_a C_b \left[\frac{dU}{dr} \right]_{r_{ad}} + \int_{r=r_{ad}}^{\infty} W(r) U(r) 4\pi r^2 dr \quad (7.5.11)$$

Applying Gauss'theorem to (7.5.11) we obtain

$$\Phi_{\infty} = 4\pi D \lim_{r \rightarrow \infty} (r^2 \, dU/dr) - \int_{r=r_{ad}}^{\infty} \left[D \operatorname{div} \operatorname{grad} U(r) - W(r)U(r) \right] 4\pi r^2 \, dr \quad (7.5.12)$$

with (7.5.8) the volume integral in (7.5.12) vanishes and Eq. (7.5.7) takes the final form [3-5]

$$\Phi_{\infty} = 4\pi D \lim_{r \rightarrow \infty} (r^2 \, dU/dr) \quad (7.5.13)$$

we define r_{eff} as [3-5]

$$r_{\text{eff}} = \lim_{r \rightarrow \infty} (r^2 \, dU/dr) \quad (7.5.14)$$

which leads with Eq. (7.5.10) to

$$r_{\text{eff}} = r_f + r_{ad} f(Z_0) \quad (7.5.15)$$

where

$$f(Z_0) \approx 0.43 Z_0^{\frac{1}{2}} K_{\frac{1}{2}}(Z_0) I_{\frac{1}{2}}(Z_0) \quad (7.5.16)$$

note that Z_0 is never going to be exactly zero, since physically α is not going to be exactly zero.

Finally the modified general expression for radiationless transfer efficiency (f_{nr}) may be written formally analogous to Eq. (3.8.3) with r_{eff} defined according to Eq. (7.5.15).

7.6 EXPERIMENTAL: COMPARISONS WITH THEORY

In this section, same experimental data reported in chapter 6 will be used again for comparisons with predictions developed from the modified model to determine its validity.

Tables 1 through 7 list these comparisons. A comparison of the theoretically calculated values for f_{nr} using our Model, with the corresponding experimental values (Tables 1-7), reveals that:

1) Our generalized Model gives much better agreement with experimental data than the previous generalized model introduced in chapter 3.

2) In most cases the Model gives almost the same results as the second Model introduced in chapter 3. It is not surprising since the effective interaction radius, r_{eff} (Eq. 7.5.15), combines both long range interaction radius (r_f) and collision radius (r_{ad}) for the second Model. If $f(Z_0) \approx 0$ (i.e. long range resonance transfer dominates),

then, $r_{\text{eff}} \approx r_f$ and the Model reduces to the second kinetics (combined diffusion and long range interactions) of the second model. On the other hand if $f(Z_0) \approx 1$ (i.e. energy transfer is mainly due to pure diffusion), then, $r_{\text{eff}} \approx r_{\text{ad}}$ and the Model reduces to the first kinetics (pure diffusion) of the second Model.

3) As the viscosity is increased, and the Forster distance, R_0 , is reduced, this Model also, as expected, underestimate the experimental data. The reason for this is that because contributions from additional terms in the dipole expansion and/or short range electron-exchange mechanisms, are not considered in the model.

Solvent \ [A] (10^{-3})		0.10	0.20	0.30	0.50	1.00	2.00	3.00	5.00
Benzene									
$n = 0.62$	f_{nr} (exp)	0.170	0.260	0.320	0.430	0.570	0.740	0.810	0.870
$R_0 = 24.2 \text{ \AA}^\circ$	Theor.	0.170	0.290	0.380	0.510	0.680	0.810	0.860	0.920
Cyclohexane									
$n = 0.98$	f_{nr} (exp)	0.160	0.270	0.330	0.430	0.590	0.750	0.800	0.880
$R_0 = 24.7 \text{ \AA}^\circ$	Theor.	0.140	0.250	0.330	0.450	0.630	0.770	0.840	0.900
B(60%), C(40%)									
$n = 1.57$	f_{nr} (exp)	0.090	0.120	0.220	0.300	0.440	0.570	0.720	0.770
$R_0 = 23.4 \text{ \AA}^\circ$	Theor.	0.080	0.140	0.200	0.300	0.460	0.630	0.720	0.820
B(30%), C(70%)									
$n = 5.89$	f_{nr} (exp)	0.050	0.080	0.150	0.190	0.300	0.440	0.520	0.650
$R_0 = 23.4 \text{ \AA}^\circ$	Theor.	0.030	0.060	0.090	0.140	0.240	0.400	0.500	0.630
B(10%), C(90%)									
$n = 25.2$	f_{nr} (exp)	0.040	0.040	0.080	0.080	0.160	0.280	0.390	0.500
$R_0 = 23.5 \text{ \AA}^\circ$	Theor.	0.014	0.028	0.042	0.069	0.129	0.234	0.318	0.447
Cyclohexanol(C)									
$n = 68$	f_{nr} (exp)	0.030	0.040	0.070	0.060	0.120	0.260	0.290	0.440
$R_0 = 23.2 \text{ \AA}^\circ$	Theor.	0.009	0.019	0.028	0.045	0.087	0.164	0.230	0.341

Table 1. Transfer quantum efficiency (f_{nr}) in naphthalene (0.1 M) - DPA [A] solutions

Solvent \ [A] (10^{-3})		2	3	4	5	7
Cyclohexane $n = 0.98$ $R_0 = 35.6 \text{ \AA}^0$	f_{nr} (exp)	0.340	0.440	0.520	0.580	0.700
	Theor.	0.410	0.530	0.620	0.680	0.760
Cyclohexanol $n = 68$ $R_0 = 34.8 \text{ \AA}^0$	f_{nr} (exp)	0.280	0.400	0.490	0.540	0.660
	Theor.	0.280	0.380	0.460	0.530	0.640

Table 2. Transfer quantum efficiency (f_{nr}) in PPO (10^{-2}) - DPA [A] solutions.

Solvent \ [A] (10^{-3})		0.313	0.625	1.250	2.500	5.000
Ethyleneglycol $n = 26.09$ $R_0 = 56 \text{ \AA}^0$	f_{nr} (exp)	16.4 \pm 3	27.2 \pm 3	47.7 \pm 6	72.0 \pm 7	81.5 \pm 9
	Theor.	0.190	0.330	0.540	0.750	0.900

Table 3. Transfer quantum efficiency (f_{nr}) in Rh6G (1.25×10^{-4} M) - Ox4 solutions

Solvent \ [A] (10^{-3})		0.313	0.625	1.250	2.500	5.000
Ethyleneglycol $n = 26.09$ $R_0 = 56 \text{ \AA}^0$	f_{nr} (exp)	15 \pm 4	20 \pm 1	41 \pm 5	64 \pm 4	81 \pm 6
	Theor.	0.170	0.310	0.510	0.720	0.880

Table 4. Transfer quantum efficiency (f_{nr}) in RhB (1.25×10^{-4} M) - NB [A] solutions.

Solvent \ [A] (10^{-3})		5	2	1
Methanol $\tau = 0.6$ $R_0 = 22.8 \text{ \AA}$	f_{nr} (exp) Theor.	0.920 0.900	0.830 0.780	0.660 0.630
Tert-Butanol $\tau = 4.8$ $R_0 = 22.4 \text{ \AA}$	f_{nr} (exp) Theor.	0.780 0.640	0.600 0.510	0.450 0.254
Glycerol $\tau = 1000$ $R_0 = 22.4 \text{ \AA}$	f_{nr} (exp) Theor.	0.390 0.242	0.280 0.108	
Cyclohexanol $\tau = 65$ $R_0 = 22.2 \text{ \AA}$	f_{nr} (exp) Theor.	0.530 0.341		
Ethyleneglycol $\tau = 17.4$ $R_0 = 23.5 \text{ \AA}$	f_{nr} (exp) Theor.	0.560 0.448		
Amylalcohol $\tau = 4.3$ $R_0 = 23 \text{ \AA}$	f_{nr} (exp) Theor.	0.770 0.710		
n-Butanol $\tau = 2.8$ $R_0 = 22.2 \text{ \AA}$	f_{nr} (exp) Theor.	0.860 0.730		
Isopropanol $\tau = 1.95$ $R_0 = 22.6 \text{ \AA}$	f_{nr} (exp) Theor.	0.840 0.790		
Ethanol $\tau = 1.2$ $R_0 = 23 \text{ \AA}$	f_{nr} (exp) Theor.	0.900 0.850		
Isobutanol $\tau = 4.1$ $R_0 = 23.2 \text{ \AA}$	f_{nr} (exp) Theor.	0.760 0.720		

Table 5. Transfer quantum efficiency (f_{nr}) in naphthalene (0.1 M) - anthranilic acid [A] solutions.

Solvent \ $[A]$ (10^{-3})		0.1	0.5	1.0	3.0	5.0
Hexane $n = 0.34$ $R_0 = 4.2 \text{ \AA}$	f_{nr} (exp)	0.020	0.080	0.155	0.355	0.480
	Theor.	0.250	0.110	0.200	0.440	0.566
Benzene $n = 0.62$ $R_0 = 4.8 \text{ \AA}$	f_{nr} (exp)	0.026	0.120	0.210	0.440	0.570
	Theor.	0.030	0.130	0.230	0.480	0.600
ISO (50%) C (50%) $n = 10$ $R_0 = 5.6 \text{ \AA}$	f_{nr} (exp)	0.010	0.050	0.090	0.230	0.330
	Theor.	0.005	0.025	0.050	0.130	0.200
Liquid paraffin $n = 172$ $R_0 = \text{ \AA}$	f_{nr} (exp)	0.005	0.020	0.040	0.120	0.180
	Theor.	0.0006	0.003	0.006	0.020	0.030

Table 6. Transfer quantum efficiency (f_{nr}) in naphthalene (0.05 M) -
Biacetyl $[A]$ solutions

Solvent \ [A] (10^{-3})		0.5	1.0	2.0	5.0
Cyclohexane $\eta = 1$ CP $R_0 = 28.2 \text{ A}^\circ$	f_{nr} (exp)	0.110	0.170	0.280	0.53
	Theor.	0.070	0.130	0.230	0.45
Mehtanol $\eta = 0.6$ CP $R_0 = 29.7 \text{ A}^\circ$	f_{nr} (exp)	0.120	0.200	0.310	0.54
	Theor.	0.090	0.160	0.290	0.53
Iso-Propanol $\eta = 2.3$ CP $R_0 = 29 \text{ A}^\circ$	f_{nr} (exp)	0.100	0.170	0.290	0.53
	Theor.	0.060	0.120	0.220	0.45
Tert-Butanol $\eta = 4.1$ $R_0 = 28.7 \text{ A}^\circ$	f_{nr} (exp)	0.090	0.200	0.300	0.50
	Theor.	0.050	0.100	0.190	0.39
Cyclohexanol $\eta = 68$ $R_0 = 27.8 \text{ A}^\circ$	f_{nr} (exp)	0.080	0.140	0.230	0.44
	Theor.	0.040	0.081	0.154	0.33

Table 7. Transfer quantum efficiency (f_{nr}) in Terphenyl (5×10^{-4} M) -
9 Methylanthracene [A] solutions

REFERENCES

- [1] WAITE. T.R, 1957, Phys. Rev. 107, 463.
- [2] FORSTER, T., 1959, Discuss. Faraday Soc., 27,1.
- [3] GOSELE. U, 1978, Spectrosc. Lett. 11, 445.
- [4] GOSELE. U, HAUSER. M, KLEIN. U.K.A, and FREY. R, 1975,
Chem. Phys. Lett. 34,519.
- [5] GOSELE. U, and HAUSER. M, 1976, Chem.Phys.Lett.41,139.

CHAPTER 8

EXPERIMENTAL: RESULTS AND ANALYSIS COMPARISONS OF THEORY AND EXPERIMENT

8.1 INTRODUCTION

In this chapter, we present and compare experimental measurements and theoretical predictions for laser gain lineshapes (and hence tunability) as well as fluorescence emission spectra in six different dye mixtures composed of (1) Dichlorofluorescein (donor) and DODC (acceptor), (2) Dichlorofluorescein (donor) and Rhodamine B (acceptor), and (3) 7-diethylamino-4 methyl coumarine (donor) and Rhodamine B (acceptor), (4) 7-diethylamino-4 methyl coumarine (donor) and Acriflavinre (acceptor), (5) Rhodamine-6G (donor) and Oxazine-4 perchlorate, and (6) Rhodamine-B (donor) and Nile Blue A perchlorate (acceptor). Four of These measurements were carried out at dye concentrations typically used for obtaining laser action.

8.2. EXPERIMENTAL: RESULT AND ANALYSIS

In the first series of experiments, two pairs of dyes were chosen such that the absorption spectrum of each acceptor dye overlapped the fluorescence spectrum of the same donor dye differently. In the experiments performed, Dichlorofluorescein was chosen as the donor, and DODC and Rhodamine B as acceptors. Ethanol was used as the solvent in cells of 1mm optical path. For excitation, the 488 nm output of an argon-ion laser was used. This line excited the donor alone. The experiment was run with both dyes in both mixtures at the same concentrations.

The first mixture consisted of Dichlorofluorescein (2×10^{-3} M/l), donor, and DODC (5.52×10^{-5} M/l), acceptor, in ethanol. The second mixture consisted of Dichlorofluorescein (2×10^{-3} M/l), donor, and Rhodamine B (5.52×10^{-5} M/l), acceptor, in ethanol.

Figs. 1 and 2 show respectively the absorption and fluorescence spectra and the overlap integrals of Dichlorofluorescein (donor) with DODC (acceptor) and Dichlorofluorescein (donor) with Rhodamine B (acceptor) in the concentrations stated above. Fig. 3 shows the experimentally determined fluorescence spectra of DODC and

Rhodamine B in each of the mixtures under the same donor excitation conditions by the argon laser. These acceptor fluorescence spectra were obtained by using the known fluorescence lineshape of the acceptors to isolate the fraction of acceptor fluorescence from total mixture fluorescence.

If energy transfer were predominantly a radiative process at the concentrations tested, energy transfer rates would be given by Eq. (2.1.1). Thus, energy transfer rate from D to A would be directly proportional to the overlap integral, P, as defined in Eq. (2.1.1). Thus, the emission from the acceptor molecules, A, would be proportional to the product of the quantum efficiency of A and the overlap integral P, as defined in Eq. (2.2.2). i.e.

$$\frac{P_1 \Phi_{o1}}{P_2 \Phi_{o2}} = \frac{\text{Fluorescence of } A_1 \text{ in mixture 1}}{\text{Fluorescence of } A_2 \text{ in mixture 2}} \quad (8.2.1)$$

Where,

A_1 = acceptor dye # 1,

A_2 = acceptor dye # 2,

$P_{1,2}$ = the overlap integrals of the fluorescence spectrum of dye, D, with the absorption spectrum of

acceptor dye, $A_{1,2}$, and $\Phi_{01,2}$ = the quantum efficiencies of the acceptor dyes $A_{1,2}$ which were experimentally determined to be 0.49 and 0.97 (in relative units) respectively.

If Eq. (8.2.1) holds, it can then be concluded that the dominant mechanism for energy transfer is by radiative process.

From Figs. 1 and 2 we obtain $P_1 = 1945$, and $P_2 = 1475$, in relative units. Inserting these values and $\Phi_{01,2}$ into the L.H.S. of Eq. (8.2.1) yields:

$$\frac{P_1 \Phi_{01}}{P_2 \Phi_{02}} = \frac{(1945) (0.49)}{(1475) (0.97)} \approx 0.666 \quad (8.2.2)$$

For the R.H.S. of Eq. (8.2.1), the fluorescence of A_1 and A_2 in the mixtures are obtained from the total area under the fluorescence curves in Fig. 3, from which: $A_1 = 117.2$ and $A_2 = 180.1$ (using the same relative units). Thus,

$$\text{R.H.S.} = \frac{117.2}{180.1} \approx 0.65$$

Showing a difference of approximately 2% with the L.H.S. This result is in conformity with radiative transfer playing the dominant role in the mixtures used.

In a second series of experiments, laser action using wideband reflectors, was obtained for two pairs of dyes (3,4). In the experiments performed, 7-diethylamino-4 methyl coumarine was chosen as the donor, and Rhodamine B and Acriflavine as acceptors. Ethanol was used as the solvent in cells of 1mm optical path. The excitation source selected for laser action in the dye mixtures was the pulsed N₂ laser output at 337.1 nm . The absorption of this pump light was predominantly by the Coumarine.

To study cw fluorescence spectra under excitation conditions similar to those with the N₂ laser source, excitation for fluorescence measurements was carried out using the 365 nm output from a Hg discharge lamp. This excitation is absorbed by Coumarine, which transfers excitation to the Rhodamine B.

The third mixture consisted of 7-diethylamino-4 methyl coumarine (10^{-3} M/litre) donor, and Rhodamine B (10^{-3} M/litre) acceptor in ethanol. Laser action using wideband reflectors, was obtained simultaneously at two wavelengths centered at 450 nm and 620 nm.

The fourth mixture consisted of 7-diethylamino-4 methyl coumarine (5×10^{-3} M/litre) donor, and Acrivlavine (10^{-4} M/litre) acceptor in ethanol. Laser action using wideband reflectors, was obtained simultaneously at two wavelengths centered at 450 nm and 490 nm.

Fig 4 shows the absorption and fluorescence spectra and the overlap integral of Coumarine with Rhodamine B for the concentrations stated above.

To further define the radiative nature of the energy transfer process involved in the third mixture, a comparison between experimental measurements for this mixture and the first two mixtures was also made, now however taking into account the various concentrations of acceptors. Thus Eq. (8.2.1) is modified to:

$$\frac{[A]_3 P_3 \Phi_{O3}}{[A]_1 P_1 \Phi_{O1}} = \frac{\text{Fluorescence of } A_3 \text{ in mixture 3}}{\text{Fluorescence of } A_1 \text{ in mixture 1}} \quad (8.2.3)$$

where,

$[A]_{1,3}$ molar concentrations of the acceptor dyes $A_{1,3}$,
 $P_{1,3}$ = the overlap integrals of the fluorescence spectrum of donor dye, $D_{1,3}$, with the absorption

spectrum of acceptor dye, $A_{1,3}$.

If Eq. (8.2.3) holds, it confirms that the dominant mechanism for energy transfer is radiative.

Inserting the appropriate terms for the third mixture (Coumarine-RhB) and the first mixture (Dichlorofluorescein-DODC) into Eq. (8.2.3) respectively yields:

$$\text{L.H.S.} = \frac{(10^{-3}) (173) (.97)}{(5.52 \times 10^{-5}) (1945) (.49)} \approx 3.189$$

$$\text{R.H.S.} = \frac{380}{117.2} \approx 3.24$$

i.e. the relationship holds, within a difference of less than 2%.

A further comparison of the third mixture (Coumarine-RhB) and the second mixture (Dichlorofluorescein-RhB) was also made. Inserting the appropriate terms for the third and second mixtures into Eq. (8.2.3) respectively yields:

$$\text{L.H.S.} = \frac{(10^{-3}) (173) (.97)}{(5.52 \times 10^{-5}) (1475) (.97)} \approx 2.12$$

$$\text{R.H.S.} = \frac{380}{180.1} \approx 2.11$$

i.e. a difference of less than 1%, again confirming radiative transfer.

Fig. 5 shows the experimental fluorescence measurements for mixture 3 with the Hg lamp excitation. It also shows the equivalent theoretical predictions using Eq. (2.2.4) assuming radiative transfer. The comparison shows excellent agreement between the experimental measurements and the theoretical predictions. Fig. 6 shows the theoretically predicted absorption and fluorescence spectra for mixture 3. Also shown is the computer generated difference between the fluorescence and absorption. This difference curve can be expected to follow the gain line shape for mixture 3, when used as a laser medium, provided the excitation source for the medium is also in the 365 nm spectral region. This is confirmed by the laser action obtained using N₂ laser excitation (at 337.1 nm) with broadband reflectors. Results shown in Fig. 6 show that as expected, lasing threshold occurs at 450 nm and 620 nm, i.e. at the peaks of the difference curve (which is equivalent to the gain line shape). Chart #1 shows the theoretical calculations for mixture 3 assuming radiative transfer.

Fig. 7 shows the experimental fluorescence measurements for mixture 4 with the Hg lamp excitation. It also shows the equivalent theoretical predictions using Eqs. (4.2.4) and (4.2.7). The comparison shows excellent agreement between the experimental measurements and the theoretical predictions.

Fig. 8 shows the theoretically predicted absorption and fluorescence spectra for mixture 4. Also shown is the computer generated difference between the fluorescence and absorption. This difference curve can be expected to follow the gain line shape for mixture 4, when used as a laser medium, provided the excitation source for the medium is also in the 365 nm spectral region. This is confirmed by the laser action obtained using N₂ laser excitation (at 337.1 nm) with broadband reflectors. Results shown in Fig. 8 show that as expected, lasing threshold occurs at 450 nm and 490 nm, i.e. at the peaks of the difference curve (which is equivalent to the gain line shape).

Note that predictions for fluorescence spectra of mixture 3 has been determined assuming that radiative transfer is the dominant mechanism, consequently Eq. (2.2.4) which only accounts for radiative transfer has

been used. On the other hand, no assumptions have been made on predicting fluorescence spectra of mixture 4, consequently Eqs. (4.2.4) and (4.2.7) which account for the general solution have been used. Chart #2 shows the theoretical calculations for mixture 4 as a general case (i.e accounting for both radiative and non-radiative mechanisms).

Comparing non-radiative transfer efficiency, f_{nr} , with radiative transfer efficiency, f_r (see chart #2), one arrive at the conclusion: total transfer efficiency, $f \approx f_r$, confirming the fact that, at the concentrations needed for lasing, radiative transfer plays the dominant role in the mixture used.

To further define the radiative nature of the energy transfer process involved in the fourth mixture, fluorescence spectra of the mixture were determined using Eq. (2.2.4), i.e. assuming radiative transfer, as expected, it were almost the same as the one obtained before using the general case.

Finally, in the last (third) series of experiments [3], two pairs of dyes (5,6) were chosen, (5) Rhodamine-6G (1.25×10^{-3} M/litre) donor and Oxazine-4 perchlorate

(1.25×10^{-3} M/litre) acceptor in glycol, and (6) Rhodamine-B (1.25×10^{-3} M/litre) donor, and Nile Blue A perchlorate (1.25×10^{-3} M/litre) acceptor in glycol. Steady-state fluorescence spectra were measured using a conventional method. Light at 530 nm was chopped and focused frontally onto the sample.

Figs. 9 and 10 show the experimental fluorescence measurements for mixture 5 and 6. It also shows the equivalent theoretical predictions using Eq. (3.4.5). The comparison shows excellent agreement between the experimental measurements and the theoretical predictions. Note that predictions for fluorescence spectra of mixtures 5 and 6 have been determined assuming that non-radiative transfer is the dominant mechanism, consequently Eq. (3.4.5) which only accounts for non-radiative transfer has been used.

In conclusion, it can be seen that knowing absorption and emission spectra in individual dyes, it is readily possible to theoretically and accurately predict fluorescence spectra of dye mixtures, where radiative or / and non-radiative processes are the dominant energy transfer mechanisms. This may be practically used to predict fluorescence of dye mixture excitation sources

[1,2]. Furthermore since the concentration regimes involved are these generally applicable to laser action, it is then also feasible and practical to predict gain lineshapes (and hence tunability) for energy transfer dye lasers. The theoretical predictions derived are generally in excellent agreement with experimental results, which confirm that at the mixture concentrations needed for lasing, radiative transfer is the dominant energy transfer mechanism.

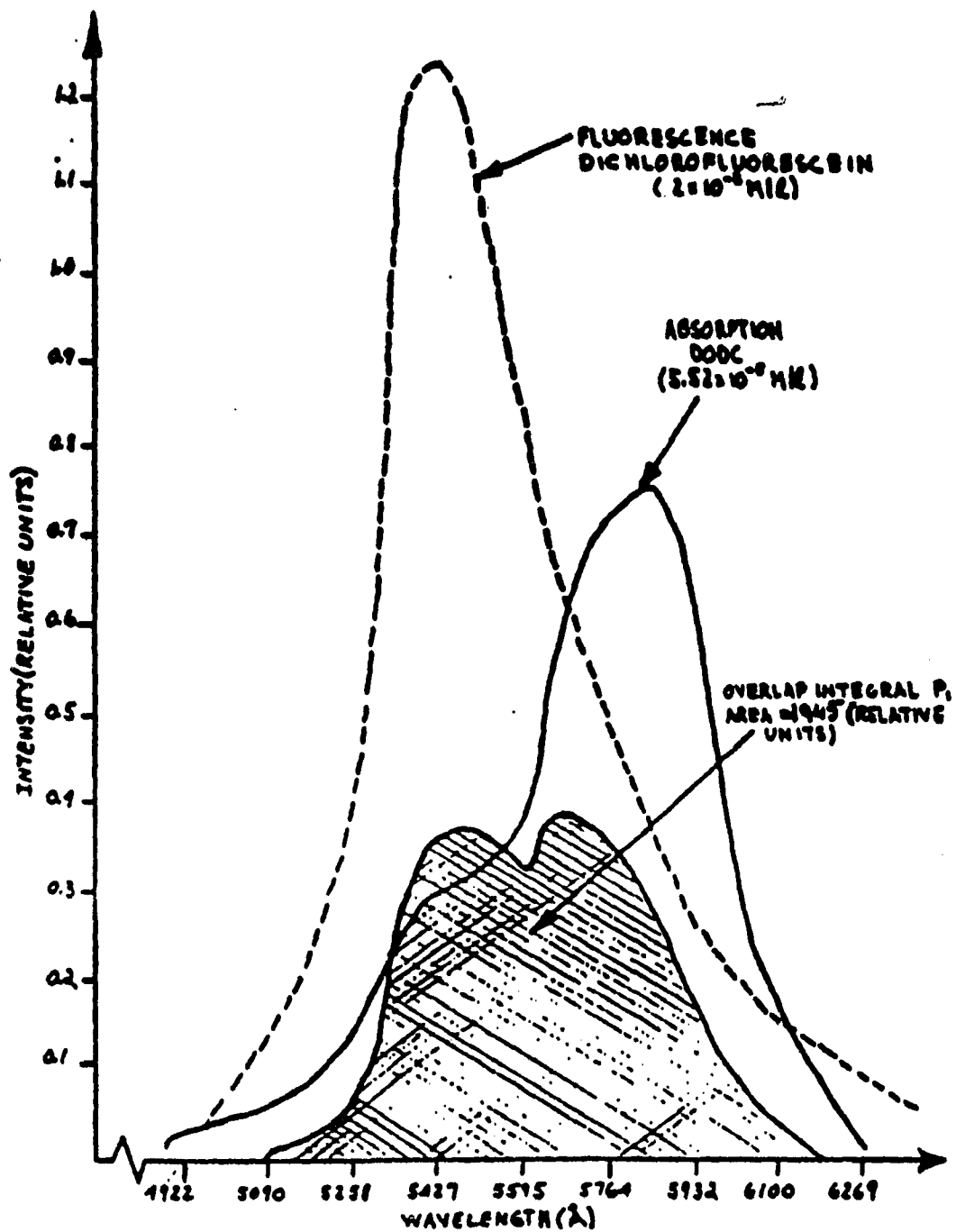


FIGURE 1 OVERLAP INTEGRAL OF DICHLOROFLUORESCIN (DONOR) AND DDC (ACCEPTOR)

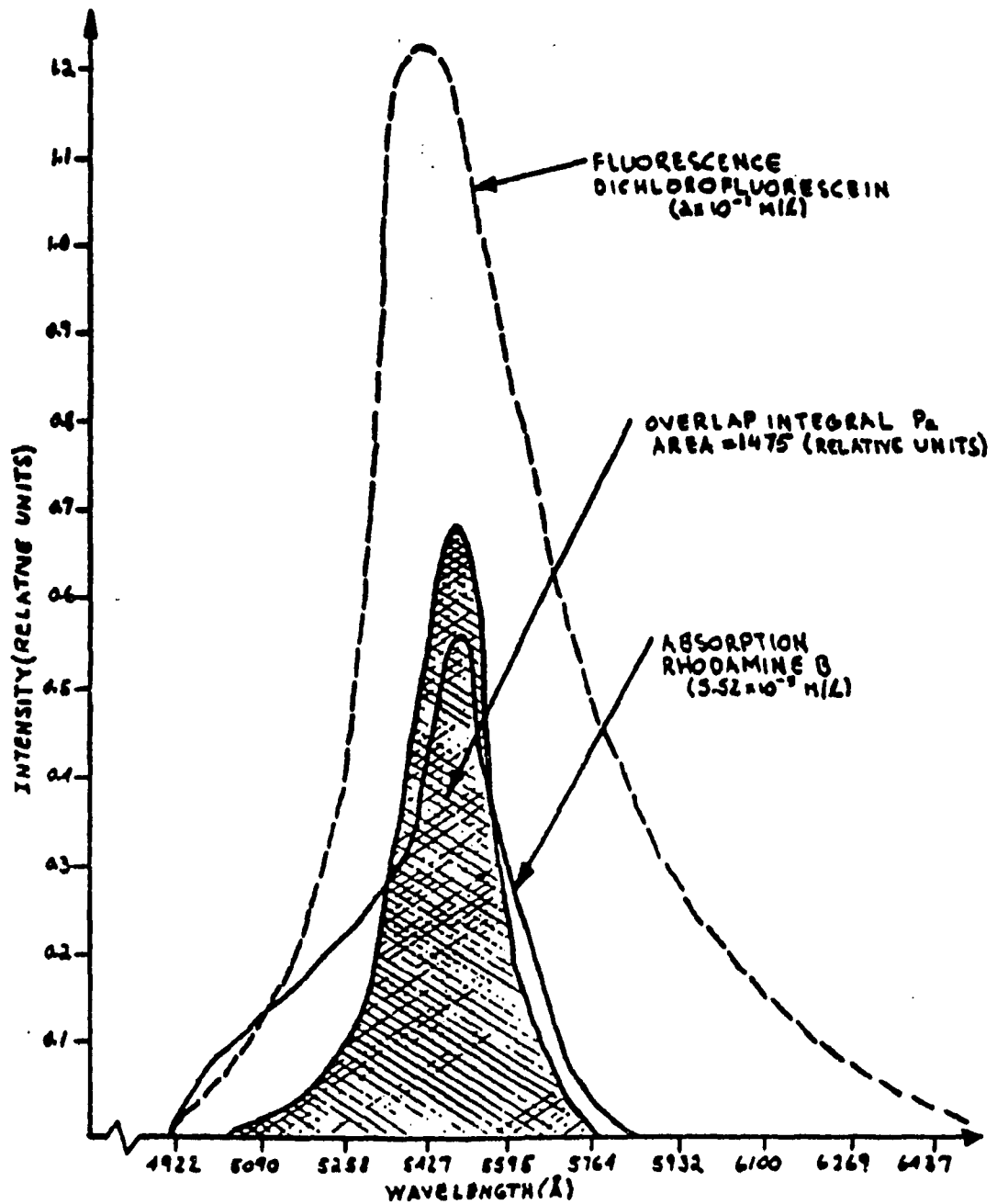


FIGURE 2: OVERLAP INTEGRAL OF DICHLOROFLUORESCEIN (DONOR) AND RHODAMINE B (ACCEPTOR)

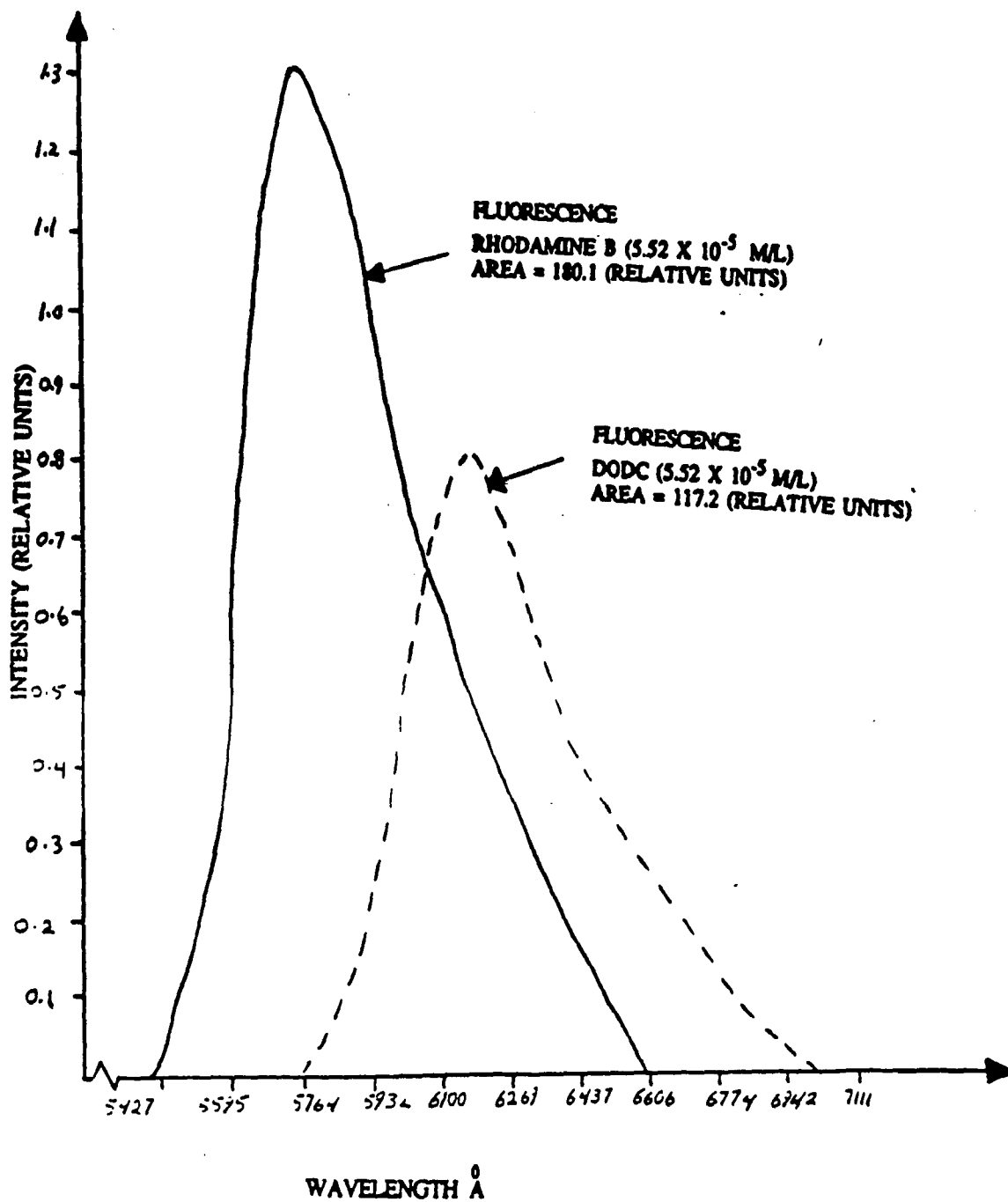


FIG.3: FLUORESCENCE YIELD OF:
 RHODAMINE B - DICHLOROFLUORESCEIN IN MIXTURE ———
 DODC - DICHLOROFLUORESCEIN IN MIXTURE - - - -

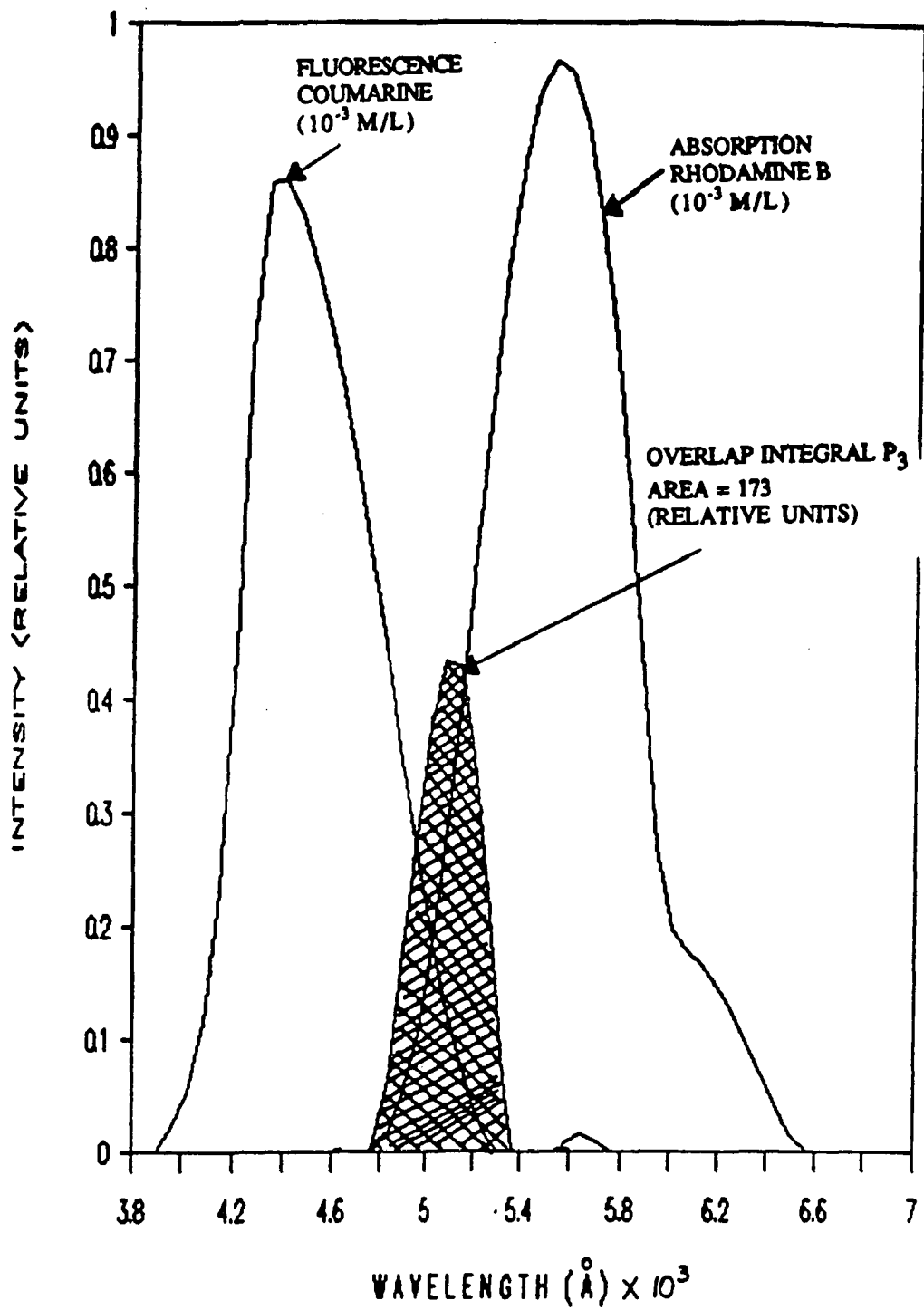


FIG. 4: OVERLAP INTEGRAL OF COUMARINE (DONOR) AND RHODAMINE B (ACCEPTOR)

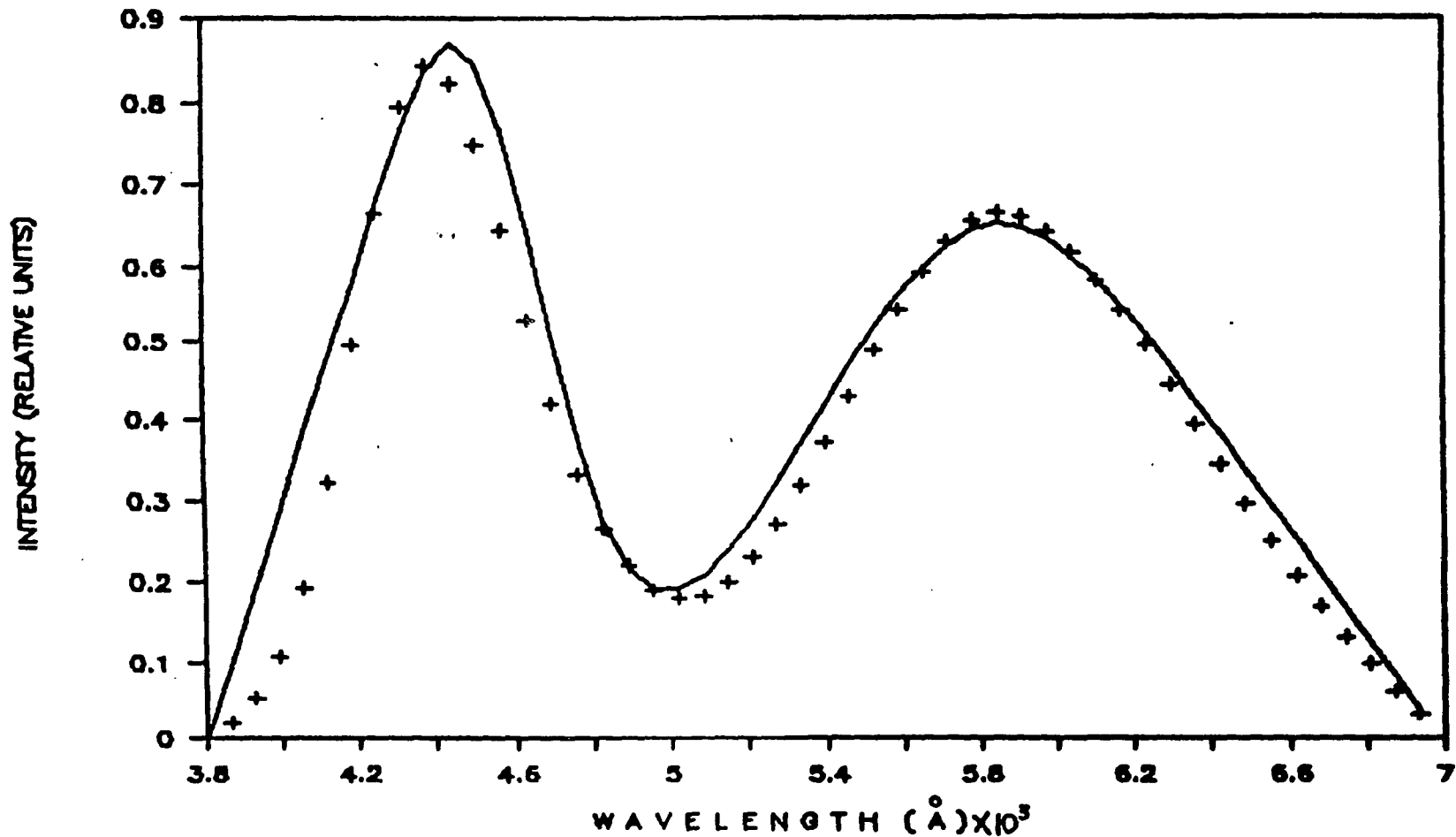


FIG. 5 FLUORESCENCE SPECTRA OF 1×10^{-3} M/L COUMARINE (DONOR) AND 1×10^{-3} M/L RHODAMINE B (ACCEPTOR) IN ETHANOL.

+++ EXPERIMENTAL

— THEORETICAL

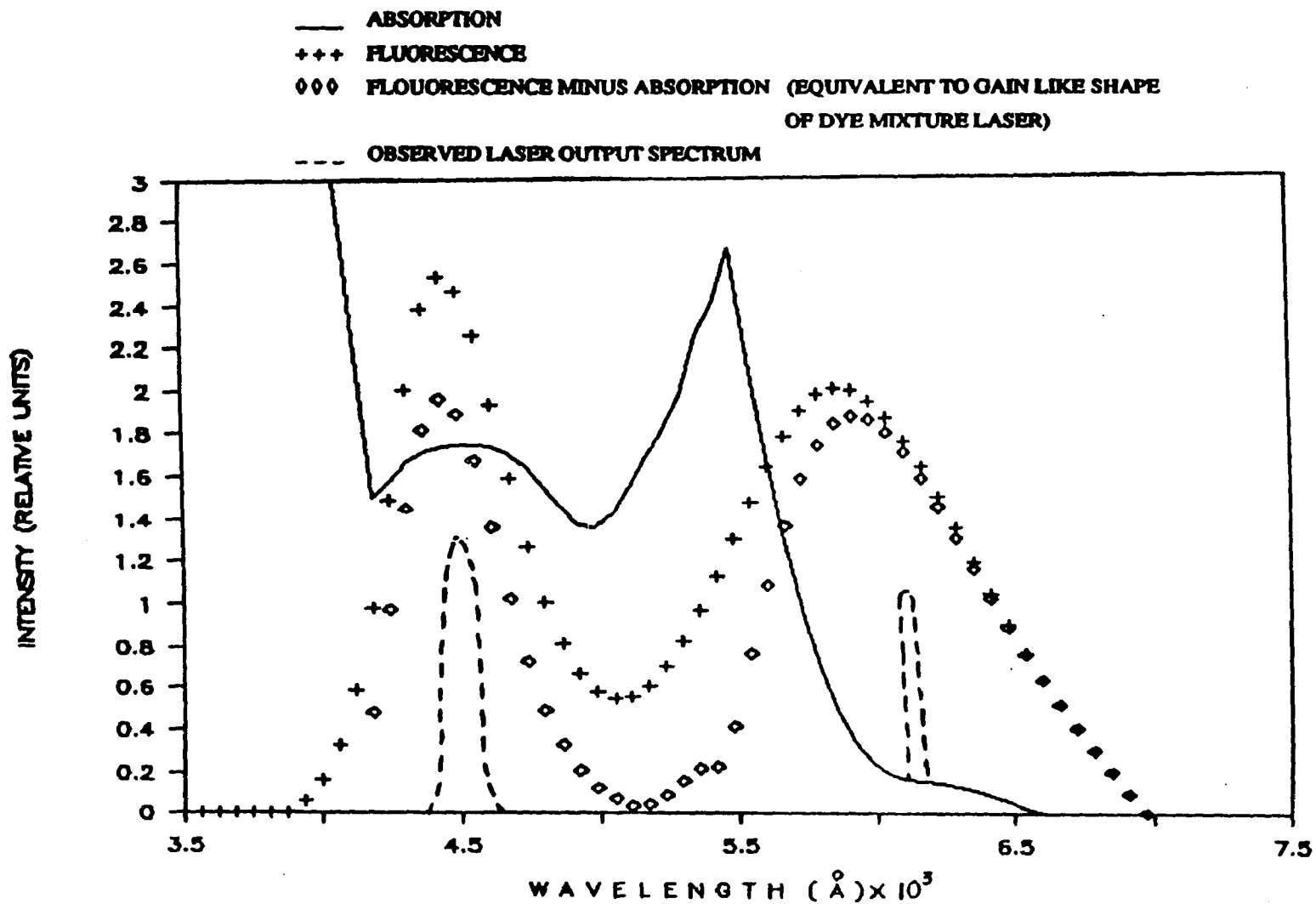


FIG. 6: PREDICTED FLUORESCENCE, ABSORPTION AND GAIN OF DYE MIXTURE:
 1×10^{-3} COUMARINE (DONOR) AND 1×10^{-3} RH-B (ACCEPTOR) IN
 ETHANOL. AND OBSERVED LASER SPECTRUM.

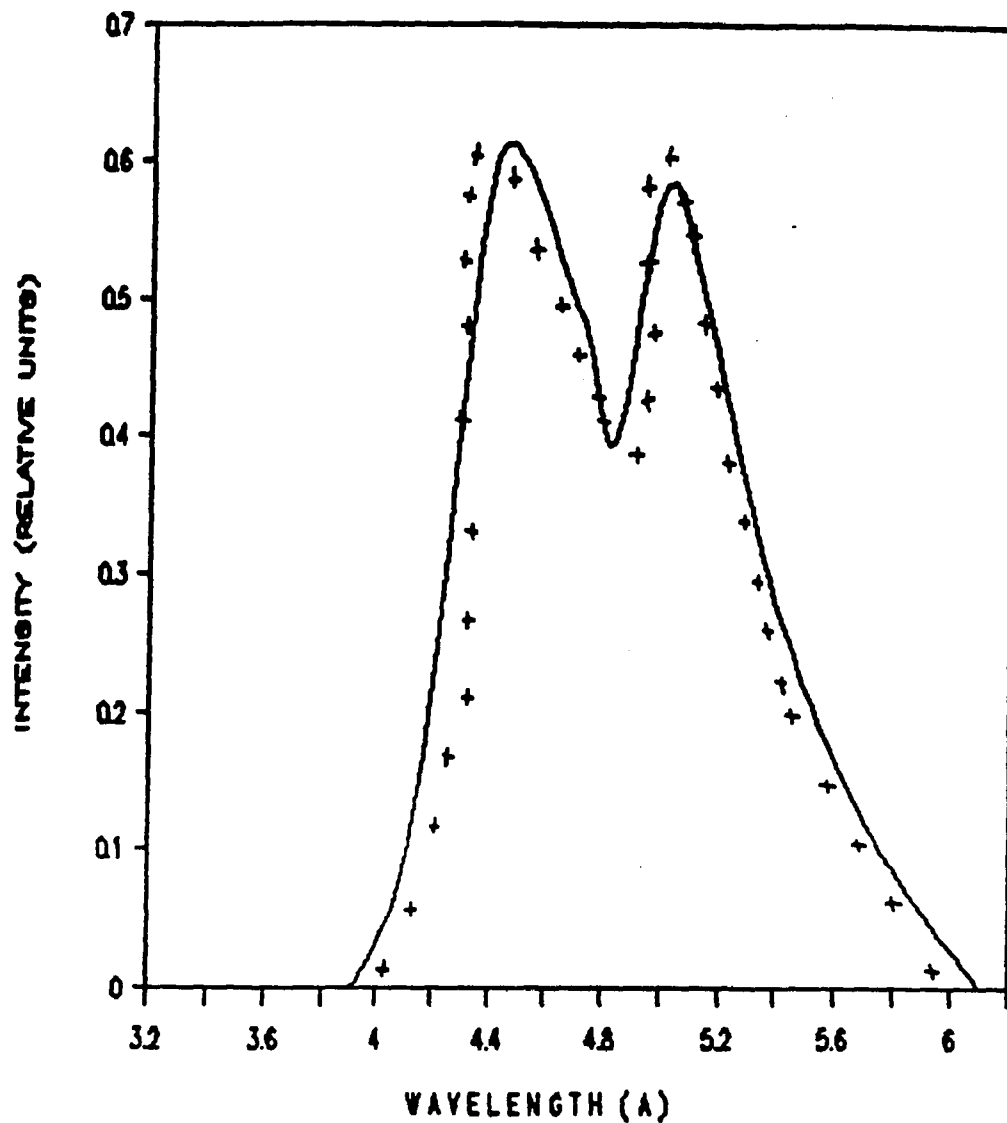


FIGURE 7: FLUORESCENCE SPECTRA OF 5×10^{-3} M/L COUMARINE (DONOR) AND 1×10^{-4} M/L ACRIFLAVINE (ACCEPTOR) IN ETHANOL.

+++ EXPERIMENTAL
 — THEORETICAL

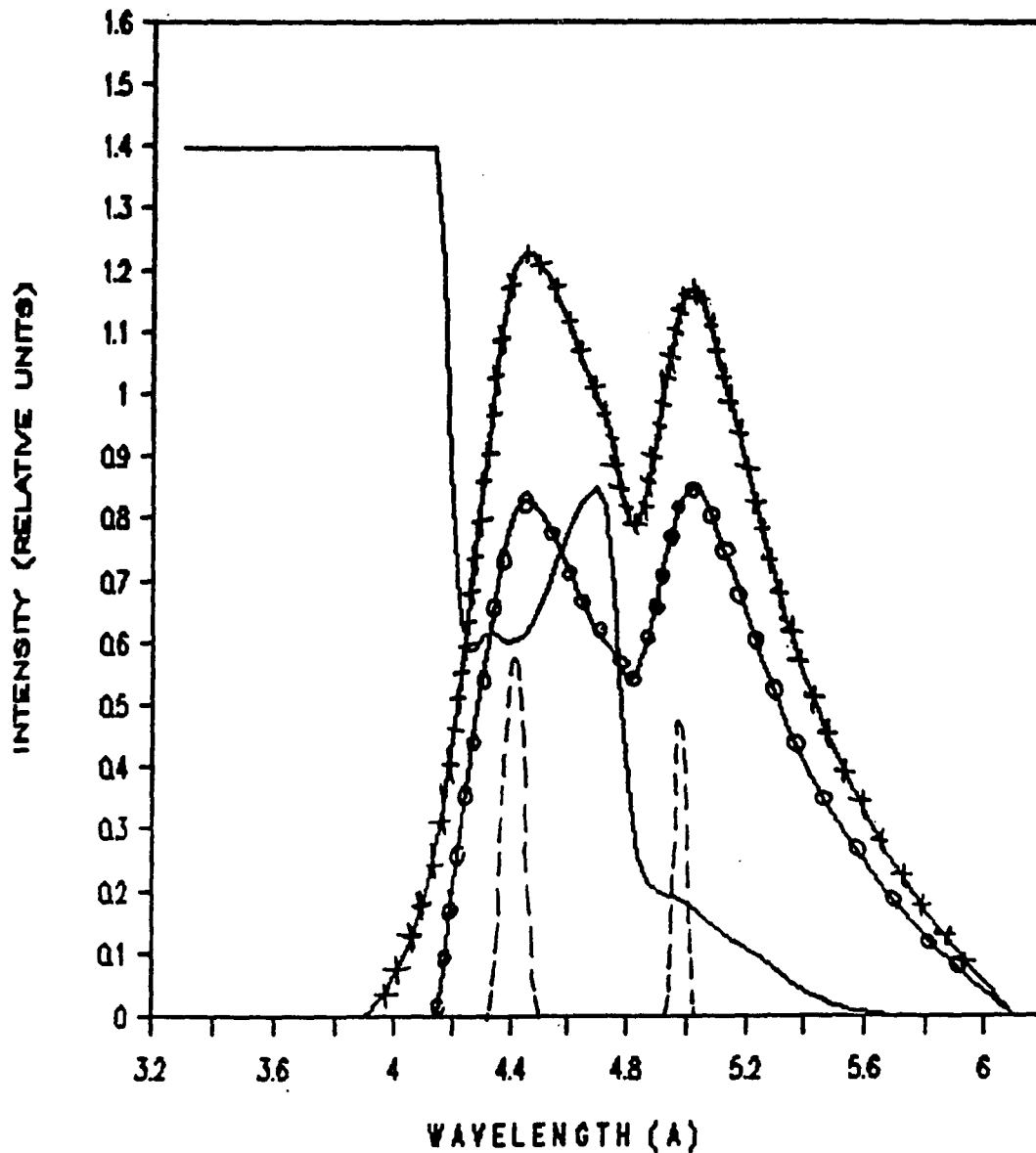


FIG. 8: PREDICTED FLUORESCENCE, ABSORPTION AND GAIN OF DYE MIXTURE:
 5×10^{-3} COUMARINE (DONOR) AND 1×10^{-4} ACRIFLAVINE (ACCEPTOR)
 IN ETHANOL. AND OBSERVED LASER SPECTRUM

— ABSORPTION
 +++ FLUORESCENCE
 ooo FLOURESCENCE MINUS ABSORPTION (EQUIVALENT TO GAIN LIKE SHAPE
 OF DYE MIXTURE LASER)
 --- OBSERVED LASER OUTPUT SPECTRUM

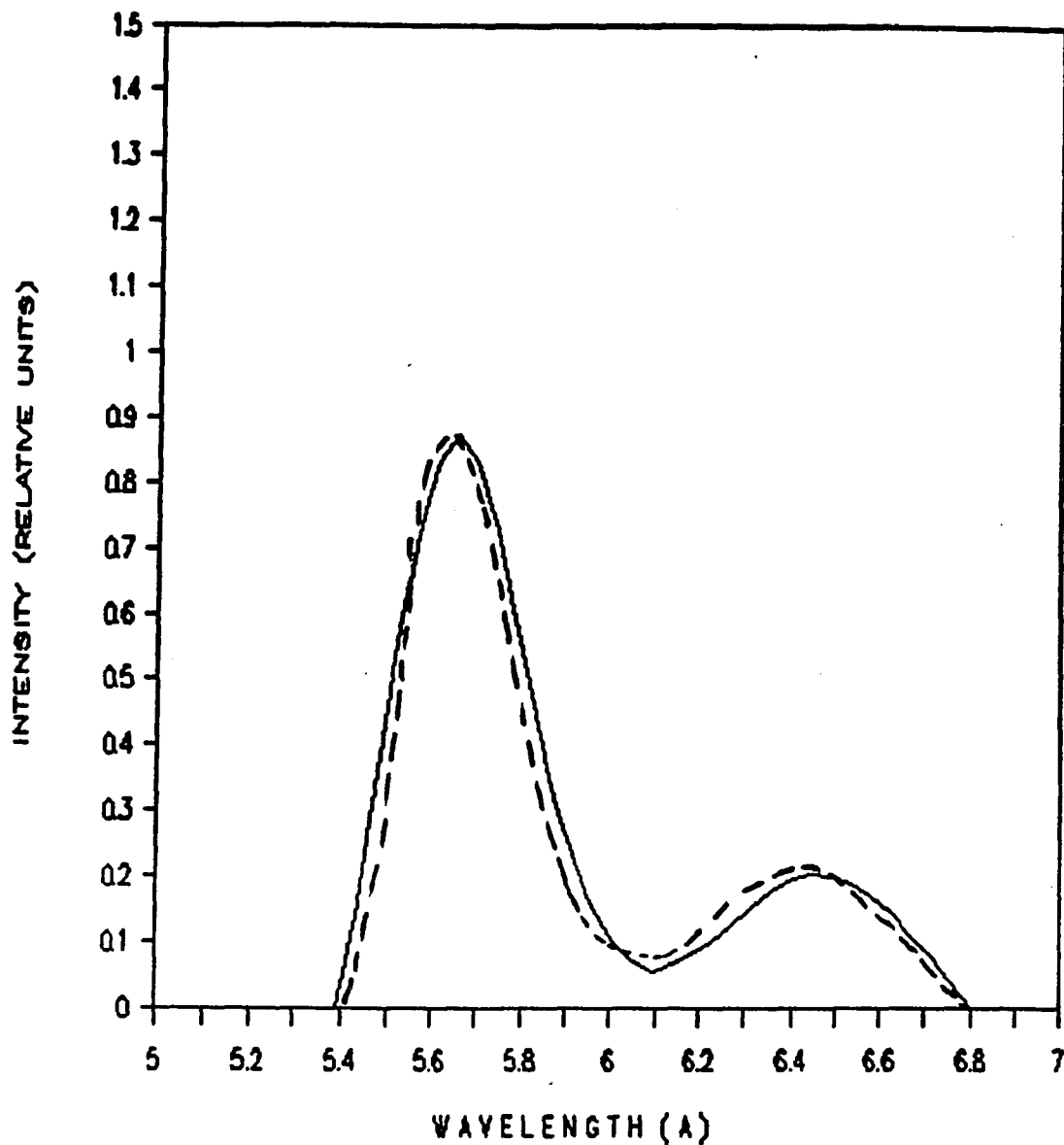


FIGURE 9: FLUORESCENCE SPECTRA OF 1.25×10^{-3} M/L R6G (DONOR) AND 1.25×10^{-3} M/L OX.4 (ACCEPTOR) IN ETHYLENE GLYCOL

- - - EXPERIMENTAL
— THEORETICAL

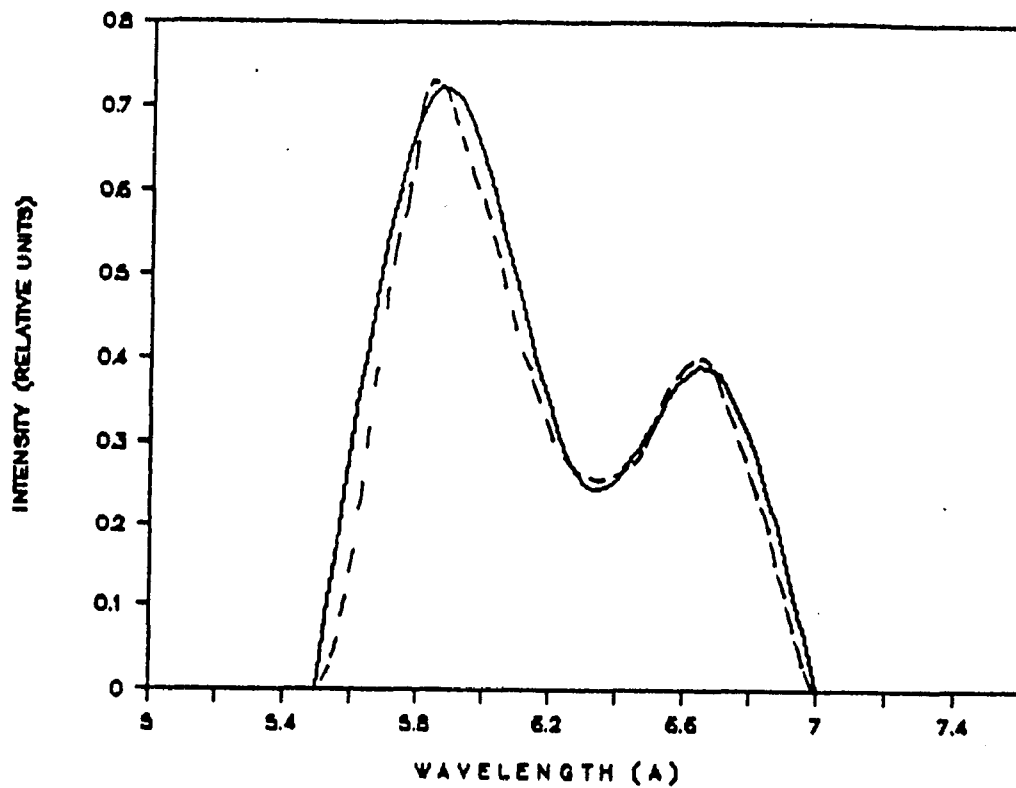


FIGURE 10: FLUORESCENCE SPECTRA OF 1.25×10^{-3} M/L RhB (DONOR) AND 1.25×10^{-3} M/L N.B. (ACCEPTOR) IN ETHYLENE GLYCOL

- - - EXPERIMENTAL
— THEORETICAL

Vessel Thickness	X = .1	Cm
Donor Concentration	[D] = .001	Moles/litre
Acceptor Concentration	[A] = .001	Moles/litre
Donor Quantum Yield	$\phi_{od} = .7$	
Acceptor Quantum Yield	$\phi_{oa} = .97$	
Donor Life Time	$T_{od} = 3E-09$	Sec
Solvent Viscosity	$\eta = 1.078$	CP
Refractive index	n = 1.3614	
Diffusion Coefficient	D = 2.037E-05	Cm ² /sec
Average distance between the Donor-Acceptor Molecules in the Solution	$R_{da} = 58.31318$	Å
Mean Molecular Diffusion Length	r = 34.96327	Å
Critical Transfer Distance	$R_o = 35$	Å

Since $R_o < R_{da}$

Energy Transfer is due to Radiative Mechanism

Area of $F_{od} = 587.2333$

Area of $F_{oa} = 447.1843$

Area of $F_d = 425.8373$

Area of $F_a = 351.3062$

Area of $F_t = 777.1435$

Fraction of the Donor Fluorescence absorbed by the acceptor

$$\alpha(\text{rad}) = 0.6167418$$

Radiative Transfer Efficiency, $f_r = \alpha \phi_{od}$

$$f_r = 0.4317193$$

CHART# 1

Vessel Thickness	X = .1	Cm
Donor Concentration	[D] = .005	Moles/litre
Acceptor Concentration	[A] = .0001	Moles/litre
Donor Quantum Yield	ϕ_{od} = .7	
Acceptor Quantum Yield	ϕ_{oa} = .8	
Donor Life Time	T_{od} = 3E-09	Sec
Solvent Viscosity	η = 1.078	CP
Refractive index	n = 1.3614	
Diffusion Coefficient	D = 2.037E-05	Cm ² /sec
Average distance between the Donor-Acceptor Molecules in the Solution	R_{da} = 42.68285	A ^o
Critical Transfer Distance	R_o = 54.05536	A ^o
Area of F_{od} = 599.783		
Area of F_{oa} = 543.1127		
Area of F_d = 206.9786		
Area of F_a = 331.1908		
Area of F_t = 538.1694		

$f_{nr} = 8.241309E-02,$	$f_r = 0.4007484,$	$f = 0.48316149$
--------------------------	--------------------	------------------

CHART #2: THEORETICAL CALCULATIONS FOR DYE MIXTURE: COUMARINE (DONOR)
AND ACRIFLAVINE (ACCPETOR) IN ETHANOL.

REFERENCES

- [1] MOREY. W. W, 1972, IEEE J. Quantum Electron. QE-8,818.
- [2] BHAWALKAR. D. D and PANDIT. L, 1973, IEEE J. Quantum Electron. QE-9, 43.
- [3] LU. P.Y, YU. Z.X, ALFANO. R.R, and GERSTEN. J.I, 1983, Phys. Rev. A 27, 2100.

SUMMARY AND CONCLUSION

The main objective of the work reported here, was to develop a theoretical approach for the operation of steady state laser dye mixtures, to permits effective basic studies to be carried out under relatively simple steady state conditions. From which theoretical predictions can be made to result in improvements of output, efficiency, and threshold pump requirements. It also permits relatively simple theoretical predictions to be made for the fluorescence of dye mixtures, and for laser gain (and hence tunability) when these mixtures are used as lasing media. To develop these expressions, a comprehensive examinations of energy transfer mechanisms in dye mixtures were needed. To carry out these examinations, theoretical models covering the main mechanisms for intermolecular energy transfer were developed. Experimental data covering a wide range of physical conditions were compared with predictions developed according to these models, to define and determine their respective validities and range of applicability. These models were shown to be appropriate to the effective analysis and handling of the dominant transfer mechanism responsible for intermolecular

energy transfer, including the selection of the most appropriate specific transfer mechanisms model for different physical conditions. Three different theoretical models were developed to predict steady state fluorescence and hence gain line shape of laser dye mixtures using computer simulation. The first model corresponds to radiative transfer, the second model corresponds to non-radiative transfer, and the third model corresponds to both radiative and non-radiative transfer mechanisms. A second set of experiments were performed on six different laser dye mixtures to measure emission spectra and lasing wavelength for each mixture. Our theoretical predictions are generally in excellent agreement with experimental results, which confirm that at the mixture concentrations needed for lasing, radiative transfer is the dominant energy transfer mechanisms.

In conclusion, it can be seen that knowing absorption and emission spectra in individual dyes, it is readily possible to theoretically and accurately predict fluorescence spectra of dye mixtures, where radiative or / and non-radiative processes are the dominant energy transfer mechanisms. This may be practically used to predict fluorescence of dye mixture excitation sources [1,2]. Furthermore since the concentration regimes

involved are these generally applicable to laser action, it is then also feasible and practical to predict gain lineshapes (and hence tunability) for energy transfer dye lasers.

One of the most important applications for future studies is to use our approach to determine the optimum concentrations required to minimize threshold pumping efficiency for laser dye mixtures.

APPENDIX

$$f_{nr} = 1 - K_0 \int_0^{\infty} \exp(-tK_0) \exp(-U [A]) dt$$

$$= 1 - K_0 \int_0^{\infty} \exp(-tK_0) \exp \left[- \left(2\pi \tilde{N} D R_0 [A] t + 4\tilde{N} R_0^2 (\pi D)^{\frac{1}{2}} [A] t^{\frac{1}{2}} \right) \right] dt$$

$$f_{nr} = 1 - K_0 \int_0^{\infty} \exp \left[K_0 + 2\pi \tilde{N} D R_0 [A] \right] t \exp \left[- \left(4\tilde{N} R_0^2 (\pi D)^{\frac{1}{2}} [A] t^{\frac{1}{2}} \right) \right] dt$$

$$= 1 - K_0 \int_0^{\infty} \exp(-K_V t) \exp(-2 A_V t^{\frac{1}{2}}) dt$$

where

$$K_V = K_0 + 2\pi \tilde{N} D R_0 [A]$$

$$A_V = 2 \tilde{N} R_0^2 (\pi D)^{\frac{1}{2}} [A]$$

Let

$$Y = \int_0^{\infty} \exp \left[- (K_V t + 2A_V t^{\frac{1}{2}}) \right] dt$$

$$\text{now } x = t^{\frac{1}{2}} \quad \Longrightarrow \quad dx = \frac{dt}{2t^{\frac{1}{2}}} = \frac{dt}{2x}$$

$$\Longrightarrow \quad dt = 2x \, dx$$

$$\begin{aligned} t=0 &\Longrightarrow x=0 \\ t=\infty &\Longrightarrow x=\infty \end{aligned}$$

$$Y = 2 \int_0^{\infty} \exp \left[- (K_V x^2 + 2A_V x) \right] dx$$

$$Y = 2 \exp(A_V^2/K_V) \int_0^{\infty} x \exp \left[- (K_V^{\frac{1}{2}} x + A_V/K_V^{\frac{1}{2}})^2 \right] dx$$

$$Y = 2 \exp(A_V^2/K_V) \int_0^{\infty} x \exp \left[\frac{K_V x + A_V}{K_V^{\frac{1}{2}}} \right]^2 dx$$

let:

$$\left[\frac{K_V x + A_V}{K_V^{\frac{1}{2}}} \right] = r$$

$$K_V x + A_V = r K_V^{\frac{1}{2}} \quad \Longrightarrow \quad dx = dr/K_V^{\frac{1}{2}}$$

$$x = \left[\frac{r}{K_V^{\frac{1}{2}}} - \frac{A_V}{K_V} \right] \quad \Longrightarrow \quad \begin{aligned} x=0 &\Longrightarrow r = A_V/K_V^{\frac{1}{2}} \\ x=\infty &\Longrightarrow r = \infty \end{aligned}$$

$$Y = \frac{2 \exp(\lambda_V^2/K_V)}{K_V^{\frac{1}{2}}} \int_{\lambda_V/K_V^{\frac{1}{2}}}^{\infty} \left[\frac{r}{K_V^{\frac{1}{2}}} - \frac{\lambda_V}{K_V} \right] \exp(-r^2) dr$$

$$Y = \frac{2 \exp(\lambda_V^2/K_V)}{K_V} \int_{\lambda_V/K_V^{\frac{1}{2}}}^{\infty} r \exp(-r^2) dr - \frac{2\lambda_V \exp(\lambda_V^2/K_V)}{K_V^{3/2}} \int_{\lambda_V/K_V^{\frac{1}{2}}}^{\infty} \exp(-r^2) dr$$

$$Y = \frac{\exp(\lambda_V^2/K_V)}{K_V} \int_{\lambda_V/K_V^{\frac{1}{2}}}^{\infty} 2r \exp(-r^2) dr - \frac{\sqrt{\pi}}{K_V^{3/2}} \lambda_V \exp(\lambda_V^2/K_V) \frac{2}{\sqrt{\pi}} \int_{\lambda_V/K_V^{\frac{1}{2}}}^{\infty} \exp(-r^2) dr$$

Let $y = r^2$

$$Y = \frac{\exp(\lambda_V^2/K_V)}{K_V} \int_{\lambda_V/K_V^{\frac{1}{2}}}^{\infty} \exp(-y) dy - \frac{\sqrt{\pi}}{K_V^{3/2}} \lambda_V \exp(\lambda_V^2/K_V) \left[1 - \operatorname{erf}(\lambda_V/K_V^{\frac{1}{2}}) \right]$$

$$Y = \frac{1}{K_V} - \frac{\sqrt{\pi}}{K_V^{3/2}} \lambda_V \exp(\lambda_V^2/K_V) \left[1 - \operatorname{erf}(\lambda_V/K_V^{\frac{1}{2}}) \right]$$

$$f_{nr} = 1 - K_0 \left[\frac{1}{K_V} - \frac{\sqrt{\pi}}{K_V^{3/2}} \lambda_V \exp(\lambda_V^2/K_V) \left[1 - \operatorname{erf}(\lambda_V/K_V^{\frac{1}{2}}) \right] \right]$$

$$f_{nr} = 1 - \frac{K_0}{K_V} + \frac{K_0}{K_V^{3/2}} \sqrt{\pi} \lambda_V \exp(\lambda_V^2/K_V) \left[1 - \operatorname{erf}(\lambda_V/K_V^{\frac{1}{2}}) \right]$$

BIBLIOGRAPHY

- AHMED. S, GERGELY. J.S, and INFANTE. D, 1974, J. Chem. Phys. 61, 1548.
- BELIKOVA. T. P, and GALANIN. M. D, 1958, Opt. Spec., 1, 168.
- BERLMAN. I.B, 1965, Handbook of fluorescence spectra of aromatic Molecules, Academic press, NEW YORK.
- BHAWALKAR. D. D and PANDIT. L, 1973, IEEE J. Quantum Electron. QE-9, 43.
- BIRKS,J.B., LEITE, M. S. S. C. P., 1970,J.Phys. B: Atom molec. Phys., 3,513.
- BIRKS,J.B., LEITE, M. S. S. C. P., 1970,J.Phys. B: Atom molec. Phys., 3,417-24.
- BIRKS. J. B, 1970, Photophysics of aromatic molecules (Willey, New York.
- BIRKS. J. B, 1948, J.Phys. B (Proc.Phys.Soc.), ser. 2, 1, 946.
- BIRKS,J.B.,and GEORGHIOUS,S.,1968,J.Phys. B (Proc. Phys. Soc.), ser.2, vol.1.
- BIRKS,J.B.,1968,J.Phys. B (Proc.Phys.Soc.),[2],1,946-57.
- BIRKS,J.B.,and CONTE,J.C.,1968,Proc.R.Soc.A,303,85-95.

BIRKS, J. B., GEORGHIOUS, S., and MUNRO, I. H., 1968, J. Phys., B
(Proc. Phys. Soc.), [2], 1, 266-73.

BUTLER. P. R, and PILLING. M. J, 1979, Chem. Phys. 41, 239.

DEXTER, D. L., 1953. J. Chem. Phys., 21, 836.

ELKANA, Y., FEITELSON, J., and KATCHALSKI, E., 1968, J.
Chem. Phys., 48, 2399-404.

FEITELSON, J., 1966, J. Chem. Phys., 44, 1500-4.

FORSTER, T., 1959, Discuss. Faraday Soc., 27, 1.

FORSTER, T., 1948, Annln. Phys., 2, 55.

GALANIN. M. D, 1955, Sov. Phys. JETP, 1, 317.

GOCHANOUR. C. R, ANDERSEN. H. C, and FAYER. M. D, 1979,
J. Chem. Phys. 70, 4254.

GOSELE. U, 1978, Spectrosc. Lett. 11, 445.

GOSELE. U, HAUSER. M, KLEIN. K. A, and FREY. R, 1975,
Chem. Phys. Lett. 34, 519.

GOSELE. U, and HAUSER. M, 1976, Chem. Phys. Lett. 41, 139.

HAAN. W, and ZWANZING. R, 1978, J. Chem. Phys. 68, 1879.

LIN. C, and DIENES, 1973, J. Appl. Phys. 44, 5050.

LU. P. Y, YU. Z. X, ALFANO. R. R, and GERSTEN. J. I, 1982,
Phys. Rev. A 26, 3610.

LU. P. Y, YU. Z. X, ALFANO. R. R, and GERSTEN. 1983, J. I, Phys.
Rev. A 27, 2100.

MOREY. W. W, 1972, IEEE J. Quantum Electron. QE-8, 818.

SEBASTIAN, P. J., 1980, Optics Commun., 35, 113.

STEINBERG. I. Z, and KATCHALSKI. E, 1968, J. Chem. Phys.,
48,2404.

TURRO. NICHOLAS. J, 1978, modern molecular photochemistry
(Benjamin,New York).

URISU, T., and KAJIYAMA, K., 1976, J. Appl. Phys., 47,
3563.

VOLTZ,R.,et al.,1966 b, J.Chim.Phys.,63,1259-64.

WAITE. T.R, 1957, Phys. Rev. 107, 463.

YOKOTA. M, and TANIMOTO. O, 1967, J.Phys.Soc. Japan, 22,
779.